Isotopes and ages in the northern Peninsular Ranges batholith, southern California

By R. W. Kistler[1], J. L. Wooden[1], and D.M. Morton[2]

Open-File Report 03-489
2003

This report is preliminary and has not been reviewed for conformity with the U.S. Geological Survey editorial standards or with the North American Stratigraphic Code. Any use of trade, product or firm names is for descriptive purposes only and does not imply endorsement by the U.S. Government.

U.S. DEPARTMENT OF THE INTERIOR
U.S. GEOLOGICAL SURVEY

[1]U.S. Geological Survey, 345 Middlefield Road (MS 937), Menlo Park, CA 94025
[2]U.S. Geological Survey, Department of Earth Sciences, University of California, Riverside, CA 92521

Isotopes and ages in the northern Peninsular Ranges batholith, Southern California

By R. W. Kistler, J. L. Wooden, and D. M. Morton

INTRODUCTION

Strontium, oxygen and lead isotopic and rubidium-strontium geochronologic studies have been completed on Cretaceous and Jurassic (?) granitic rock samples from the northern Peninsular Ranges batholith in southern California. Many of these samples were collected systematically and studied chemically by A. K. Baird and colleagues (Baird and others, 1979). The distribution of these granitic rocks is shown in the Santa Ana, Perris, and San Jacinto Blocks, bounded by the Malibu Coast-Cucamonga, Banning, and San Andreas fault zones, and the Pacific Ocean on the map of the Peninsular Ranges batholith and surrounding area, southern California (Figure 1). The granitic rock names are by Baird and Miesch (1984) who used a modal mineral classification that Bateman and others (1963) used for granitic rocks in the Sierra Nevada batholith. In this classification, granitic rocks have at least 10% quartz. Boundaries between rock types are in terms of the ratio of alkali-feldspar to total feldspar: quartz diorite, 0-10%; granodiorite, 10-35%; quartz monzonite 35-65%; granite>65%. Gabbros have 0-10% quartz.

Data for samples investigated are given in three tables: samples, longitude, latitude, specific gravity and rock type (Table 1); rubidium and strontium data for granitic rocks of the northern Peninsular Ranges batholith, southern California (Table 2); U, Th, Pb concentrations, Pb and Sr initial isotopic compositions, and $\delta^{18}O$ permil values for granitic rocks of the northern Peninsular Ranges batholith (Table 3).

Locations of samples investigated for this report are shown on Figure 2: specimens chemically analyzed (Baird and others, 1979, open circles), specimens from a west to east age and isotopic traverse across the northern part of the area (Premo and others, 1997, open hexagons), and specimens with initial $^{87}Sr/^{86}Sr$ determined for a test of displacement along the San Andreas fault (Kistler and others, 1973, open squares).

ANALYTICAL METHODS

The rubidium and strontium concentration and Sr isotopic data reported in Table 2 were gathered in the Sr isotope laboratory at the USGS in Menlo Park, California. Results are presented here for aliquots of whole-rock powders prepared for determination of major and trace element chemical compositions reported elsewhere. Rubidium and strontium abundances were determined by energy dispersive X-ray fluorescence methods. Concentrations of Rb and Sr by X-ray fluorescence are ± 3%. Strontium isotope ratios were determined using a MAT 261, 90° sector mass spectrometer, using the double rhenium filament mode of ionization. Strontium isotopic compositions are normalized to $^{86}Sr/^{88}Sr=0.1194$. Measurements of NBS strontium carbonate standard SRM 987 yield a mean $^{87}Sr/^{86}Sr$ of 0.710239±0.000015 over the period of the study (04/03/92 – 05/09/92). Analytical uncertainties in $^{87}Sr/^{86}Sr$ values are about ±0.008%.

In Table 2, measured $^{87}Sr/^{86}Sr$ values are reported to five places and are routinely measured precisely to ± 2 in the fifth place, whereas initial $^{87}Sr/^{86}Sr$ values are reported to four places. The initial strontium isotopic values of single plutonic rock samples are probably *accurate* to only ± 5 in the fourth place; either because of possible variability observed in multiple samples from plutons, or also because of lack of precise ages used to calculate these values in some samples. An assigned age of 100 Ma was used to calculate initial $^{87}Sr/^{86}Sr$

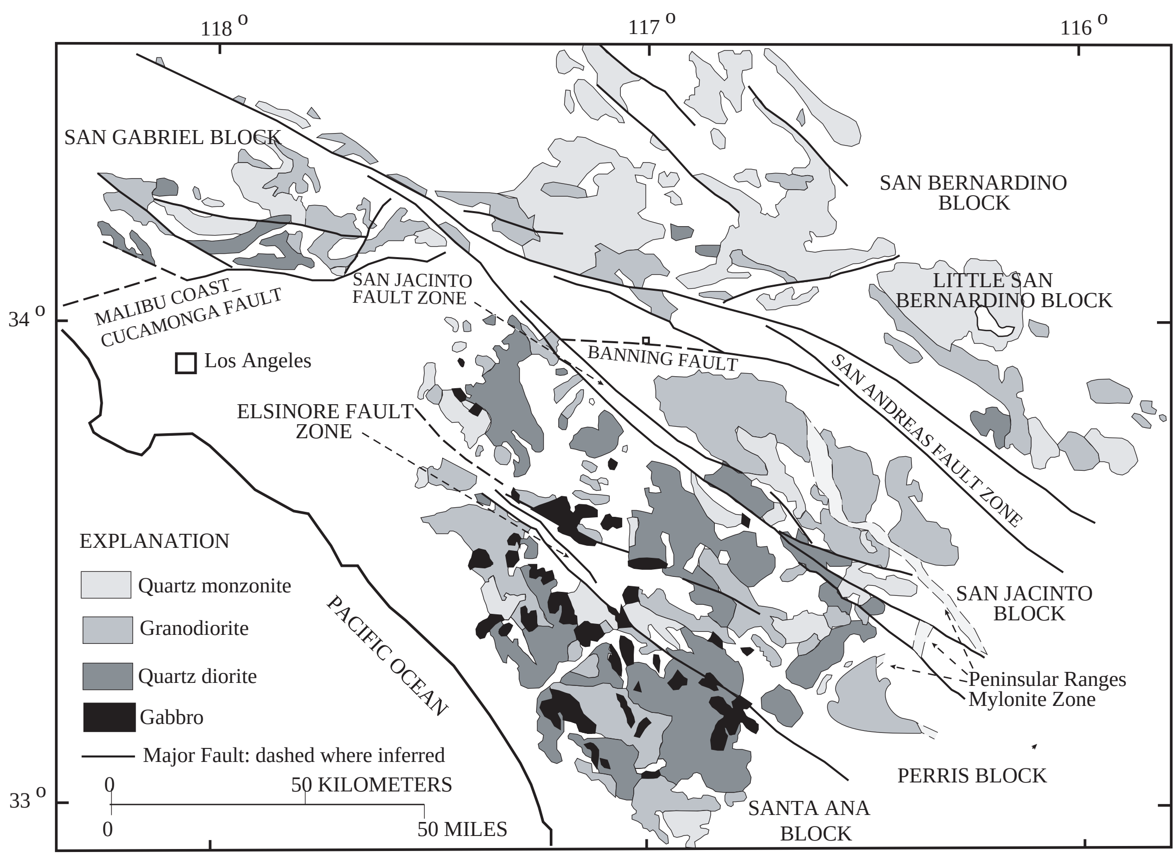

Figure 1. Pluton map of the Peninsular Ranges batholith and surrounding area, southern California (from Baird and Miesch, 1984).

values for those specimens without any age control by either U-Pb zircon dates or Rb-Sr whole-rock isochron dates. Ages followed by “Z” or by “R” (Table 2, Age column) indicate they are assigned from zircon U-Pb data or by Rb-Sr whole-rock isochrons, respectively. The initial $^{87}Sr/^{86}Sr$ values reported for whole-rocks, and whole-rock Rb-Sr isochron ages reported in Table 2 were calculated using the decay constant for rubidium from Steiger and Jager (1977) and the ISOPLOT program of Ludwig (1999).

Oxygen was extracted from whole-rock samples by the BrF_5 method (Clayton and Mayeda, 1963) or by ClF_3 method (Bothwick and Harmon (1982) in nickel bombs at 550°C and converted to CO_2 by reaction with hot carbon. The CO_2 was analyzed on a MAT-251 isotope ratio mass spectrometer. Extractions and analyses of oxygen were done in the USGS stable isotope laboratory in Menlo Park, California. All of the $\delta^{18}O$-values reported in Table 3 were analyzed in duplicate with reproducibility of $\delta^{18}O$ of ± 0.15 permil or better relative to the SMOW standard.

Pb isotope compositions (Table 3) were determined in the laboratory at the U.S. Geological Survey in Menlo Park for aliquots of the same whole-rock powders used for Rb, Sr, and $\delta^{18}O$ determinations. Pb was separated from the whole-rock powder using standard anion exchange processes uusing HBr and HCl. Pb isotopic compositions were determined in static-collection mode on a MAT 262 mass spectrometer. Thermal fractionation is monitored by running NBS-981 and –982 standards. The empirically determined fractionation correction factor is 0.0011 per mass unit and its uncertainty is the largest contribution to the total analytical uncertainty of about 0.1% associated with the Pb isotopic ratios.

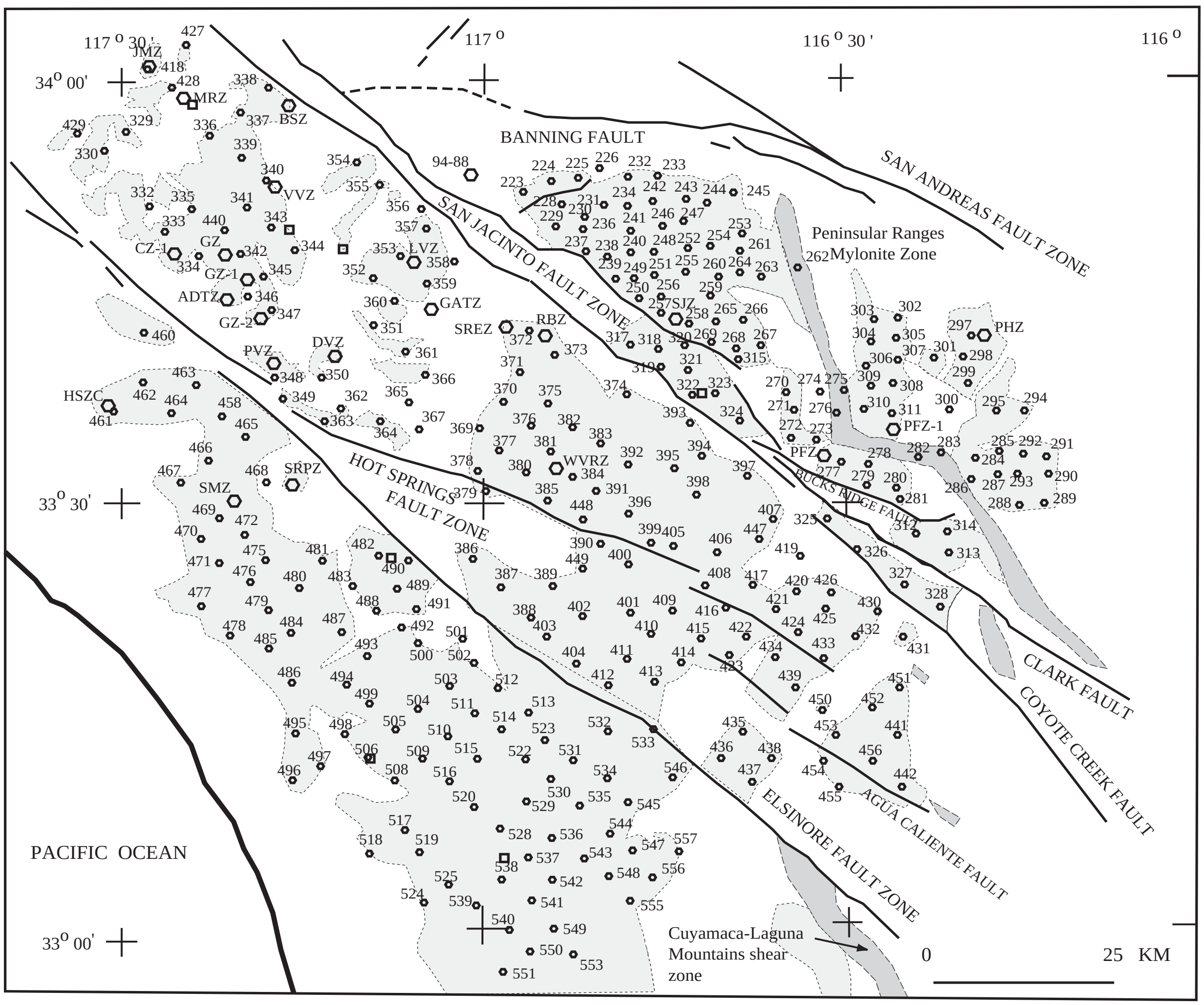

Figure 2. Map showing exposures of granitic rocks (light gray), major faults (from Rogers, 1965), locations and specimen numbers of granitic rocks investigated in the northern Peninsular Ranges batholith. Symbols: circles (Baird and others, 1979); hexagons (Premo and others, 1997), squares (Kistler and others, 1973).

The measured Pb isotopic compositions have been combined with U, Th and Pb concentrations for these samples (Lichte, 1994; Wooden and others, 1994) and crystallization age data (Table 2) to calculate initial Pb isotopic values. Pb isotope initial ratios calculated from whole-rock samples have a higher uncertainty than those measured in feldspar mineral separates. This is because of the analytical uncertainties associated with the U and Th concentrations, and the susceptibility of medium- and coarse-grained granitic rocks to loss of U in surficial weathering environments. The most common error in initial Pb ratios calculated from whole-rock powders is for the present-day $^{206}Pb/^{204}Pb$ values to be under-corrected because the measured U concentration is too low as a result of U-loss during weathering. The $^{206}Pb/^{204}Pb$ ratio experiences the most change in Phanerozoic materials because of the very high ratio of ^{238}U to ^{235}U for this time interval.

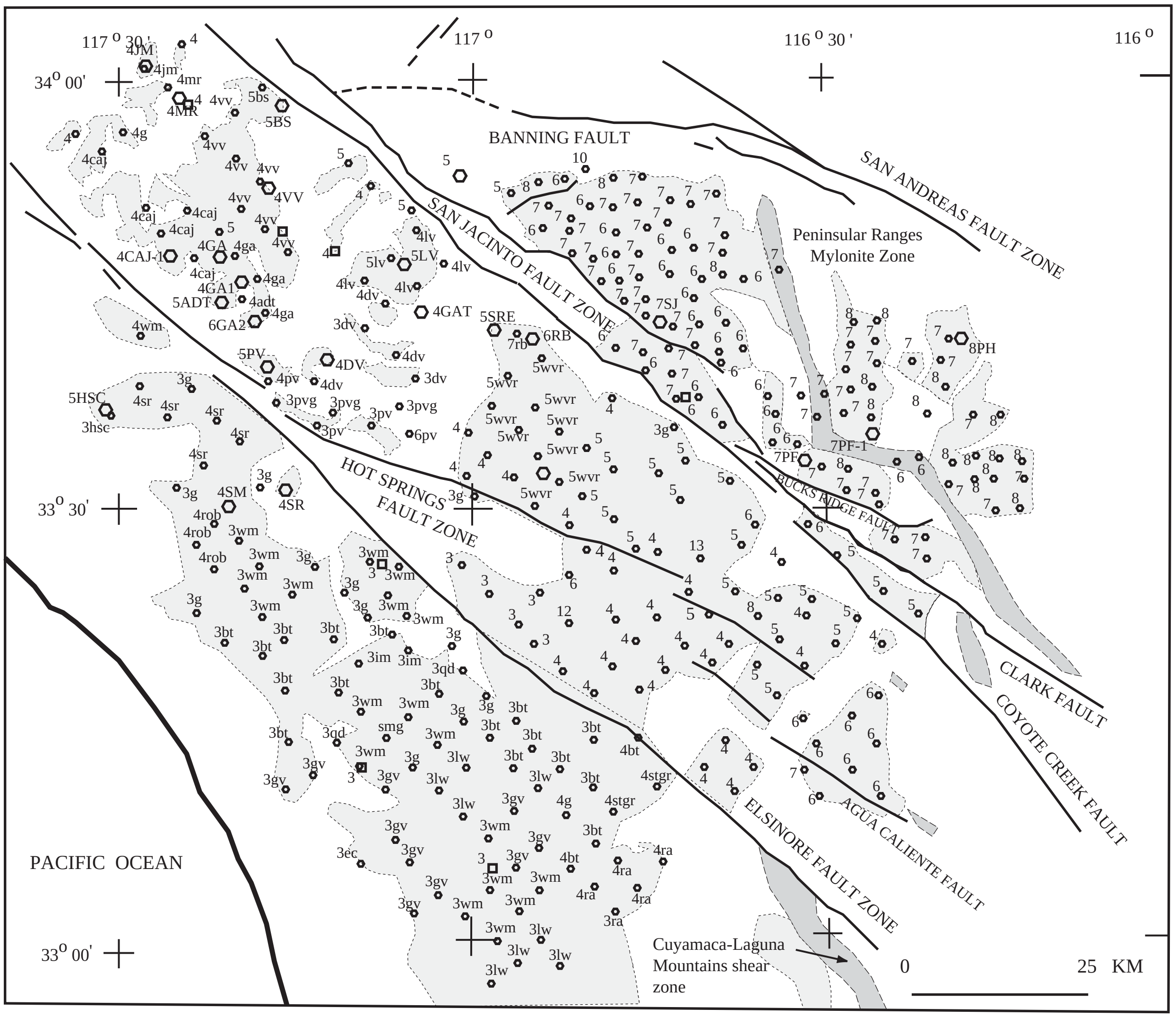

Figure 3. Sample locations and initial $^{87}Sr/^{86}Sr$ values for granitic rocks in the northern Peninsular Ranges. Sri Values are: 3=0.7030-0.7039; 4=0.7040-0.7049; 5=0.7050-0.7059; 6=0.7060-0.7069; 7=0.7070-0.7079; 8=0.7080-0.7089. Pluton names, where known, are indicated by initials after the Sri values. Symbols: Santa Ana block: lw, Lake Wolford; ra, Ramona ring dike; wm, Woodson Mountain; bt, Bonsall; gv, Green Valley; stgr, Stonewall; rob, Roblar; g, gabbro; im, Indian Mountain; HSC, Hot Springs Creek; SR, Santa Rosa; SM, Squaw Mountain; Perris block: JM, Jurupa Mountain; MR, Mount Rubidoux; BS, Box Springs; VV, Val Verde; CAJ, Cajalco; GA, Gavilan; ADT, Arrroya del Torro; LV, Lakeview Mountain; GAT, Green Acres;

DV, Domenigoni Valley; SRE, Searles Ridge; RB, Ramona Bowl; WVR, Wilson Valley; PV, Paloma Valley. San Jacinto block: SJ, San Jacinto; PF, Pinyon Flat; PH, Point Happy.

ISOTOPIC DATA

Rb and Sr abundances, measured $^{87}Sr/^{86}Sr$, initial $^{87}Sr/^{86}Sr$ (Sri) values, and known or estimated ages for all available sample powders are given in Table 2. Sri values of each specimen are shown on a map of their locations in Figure 3. Sample location symbols are the same as those in Figure 2, and each location has a number that represents the last or least significant digit of the Sri of the granitic rock from that locality, when truncated at 3 significant digits. About half of the locations have a Sri value followed by letters that represent the name of a mapped pluton at that location. The abbreviated names are identified in Table 2 and Figure 3. The numbers at each location represent the 3rd place of the Sri value calculated for each sample. For example 3wm represents Sri in the range 0.7030-0.7039 and the rock is Woodson Mountain granodiorite of Larsen (1948), whereas 4lv represents a Sri is in the range 0.7040-0.7049 and the rock is Lakeview Mountain tonalite of Dudley (1935).

Oxygen isotope values (as $\partial\ ^{18}O$) determined for about one-third of the samples available are given in Table 3 and plotted on Figure 4. Measured values range from 2.3 to 12.8 per mil and most represent primary, magmatic values for these specimens. However, in the southern part of the Santa Ana block (Figure 4), sample $\partial\ ^{18}O$ values range from 2.3 to 6.9 and the lower values probably identify rocks altered by a cell of low ^{18}O meteoric hydrothermal water. Taylor and Silver (1978) identified similar hydrothermally altered granitic rocks extending from Ensenada, Baja California to Riverside, California in the western exposures of the southern California batholith.

Whole-rock age corrected initial $^{206}Pb/^{204}Pb$, $^{207}Pb/^{204}Pb$, and $^{208}Pb/^{204}Pb$ values for plutons in the northern Peninsular Ranges batholith are given in Table 3 and initial $^{206}Pb/^{204}Pb$ values are plotted on a map of their locations in Figure 5. Values of ^{206}Pb /^{204}Pb in the Peninsular Ranges batholith range from about 18.4 to 19.5. Values of ^{208}Pb/ ^{204}Pb range from about 38.1 to to 39.0 and $^{207}Pb/^{204}Pb$ range from 15.57 to 15.72.

STRONTIUM AND OXYGEN ISOTOPE BOUNDARIES

Taylor and Silver (1978) identified a remarkably straight northerly trending boundary marked by a step between $\partial\ ^{18}O$ values less than 8.5 permil to the west and greater than 9.0 permil to the east in plutonic rocks of the Peninsular Ranges batholith from southern California into Baja California. The northerly trending dashed line in Figure 4 shows the oxygen isotope boundary between the western and eastern Peninsular Ranges batholith ($\delta\ ^{18}O<9.0$ and >9.0 permil, respectively) identified by our data in this area. This isotopic boundary lies within a major geologic boundary identified by Larsen, (1948) and Gastil (1975) that divides the batholith into western, epizonal to mesozonal granitic rocks and abundant gabbros from eastern, more deep-seated granitic rocks and few gabbros. It also lies within a diffuse geophysical boundary identified by Bouger gravity (Oliver, 1980), isostatic residual gravity (Roberts and others, 1990), aeromagnetic anomalies (Jachens and others, 1991), regional crustal thickness (depth to Moho, Lewis and others, 2000), crustal seismic velocities (Hauksson, 2000), and p-wave velocity image (Magistrale and Saunders, 1995). Defined bt these parameters, this boundary divides the Peninsular Ranges batholith into eastern (EPRB) and western segments (WPRB).

Early and Silver (1973) and Kistler and others (1973) reported the first reconnaissance strontium isotopic studies of plutons in the northern Peninsular Ranges batholith. Both studies showed a southwest to northeast variation of Sri from about 0.703 to 0.708. Hill and Silver (1988) reported a detailed study of strontium isotopic heterogeneity in the San Jacinto pluton in the San Jacinto block (Figure 1) of the batholith. Gromet and Silver (1987) drew isopleths of Sri (0.704, 0.706) along the length of the northern 600 km of the batholith.

Kistler and Morton (1994) and Morton and Kistler (1997) gave preliminary discussions of Sri of specimens collected by Baird and others (1979) between 33 and 34 degrees North Latitude (Figure 3) that provide the most detailed pattern of variation in Sri for granitic rocks in any part of the Peninsular Ranges batholith. Their results are summarized and shown by Sri isopleths along with the oxygen isotope boundary from Figure 4 on the outline map of granitic rock exposures on Figure 6.

Plutons in the Santa Ana block have a simple Sri pattern (Figure 3). The data define two 0.704 isopleths (Figure 6). A northern isopleth trends SW-NE and separates the Woodson Mountain granodiorite of Larsen (1948) from the Roblar leucogranite of Larsen (1948) and the Santa Rosa, Squaw Mountain, and Hot Springs Canyon plutons of this report (Figure 3). A southern isopleth trends N-S and is the boundary between Woodson Mountain granodiorite, Lake Wolford granodiorite, and Bonsall tonalite to the west, and the Ramona ring complex (Merriam, 1941) and related outliers to the east (Figure 3). This Sri isopleth is parallel to, but about 10 kilometers west of the 9.0 $\delta^{18}O$ isopleth in the area. Together, these northerly trending isotopic boundaries lie within the diffuse northwest trending boundary recognized along the length of southern and Baja California that separates the western from the eastern Peninsular Ranges batholith. The diffuse boundary between magnetite-series and ilmenite-series granitic rocks (Diamond and others, 1985, Gastil, 1990) also coincides with the geological and geophysical separation of western from eastern plutons of the batholith.

The sinuous eastern limit of plutons sampled by Baird and others (1979) in the Santa Ana block (figure 6) is the western margin of the granodiorite of Cuyamaca Reservoir, an intrusive unit that is interlayered with prebatholithic schist (Todd and Shaw, 1985). Todd and Shaw (1985) report Sri values from 0.7079 to 0.7098 and $\partial^{18}O$ values from 11.8 permil to to 13.8 permil for this pluton and classify it as a S-type granitoid. This boundary marks their I-S line in the Santa Ana block.

Plutons in the Perris block have a more complex and greater range of Sri than shown by our data in the Santa Ana block (Figure 6). Most of the values fall between 0.703 and 0.706, but there are scattered values of some isolated samples from 0.706 to as high as 0.713 (Figure 3). The 0.704 isopleth (Figure 6) is north trending and located about 10 km west of the 9.0 $\delta^{18}O$ isopleth. However, to the north of the Hot Springs fault zone, where it meets the tectonic boundary of Morton and Gray (2002), the 0.704 isopleth turns to the west across the northern part of the block until it is truncated by the Elsinore fault zone.

A 0.705 isopleth trends south from the San Jacinto fault zone to the right angle bend in the 0.704 isopleth and then trends southeast to the Hot Springs fault zone. Here, the fault zone is the 0.705 isopleth. A second 0.705 isopleth is parallel to the San Jacinto fault zone and extends from the Box Springs pluton southeast to the Lakeview Mountains Pluton.

A 0.706 isopleth is drawn in mixed metamorphosed sedimentary rocks and granitic rocks along San Ysidro Mountain. This isopleth separates the easternmost pluton sampled (T=104.4±7.5Ma, Sri=0.7062, Table 2), here called the granodiorite of Pinyon Ridge, from other plutons (Sri less than 0.706) to the west in the Perris block (Figure 6). The eastern exposures of the granodiorite of Pinyon Ridge, is the Borrego Springs shear-zone section of the Peninsular Ranges Mylonite Zone (Figure 1, Simpson, 1984). Field evidence indicates this segment of the mylonite zone is a post-mid-Cretaceous west directed thrust (Simpson, 1984) complicated by Miocene detachment faulting (Engel and Schultejann, 1984), and the granodiorite of Pinyon Ridge is below the thrust and detachments.

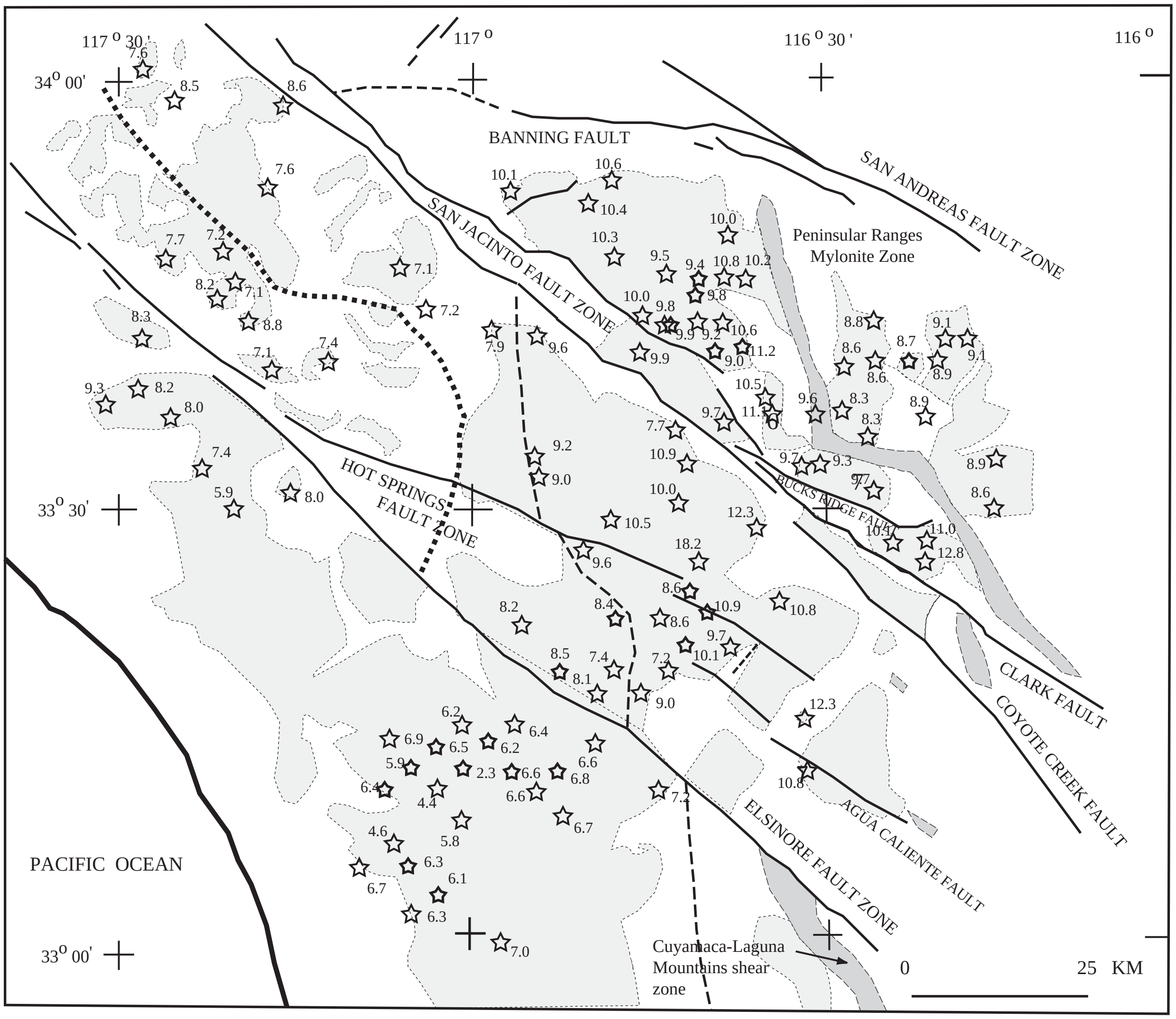

Figure 4. Specimen locations and $\delta^{18}O$ values in the northern Peninsular Ranges batholith. Northerly trending dashed line separates $\delta^{18}O$ values greater than +9.0 permil and less than +9.0 permil. Heavy dotted line in the northern Perris block is a tectonic boundary that separates undeformed shallow level plutons to the southwest from deformed deep level plutons to the northeast (Morton and Gray, 2002).

Two other 0.706 isopleths are defined close to the San Jacinto fault zone. The first by specimens from the Ramona Bowl pluton (Sri>0.706) and the second by specimens B407 west of the Coyote Creek segment of the San Jacinto fault zone (Figures 2, 6). We note here that specimens

B407and B325 are almost identical in Rb and Sr concentrations, measured $^{87}Sr/Sr$, and Sri (0.7066) at 100 Ma. Specimen B325 is adjacent to B 407, but east of the Coyote Creek segment of the San Jacinto fault zone (Figure 2).

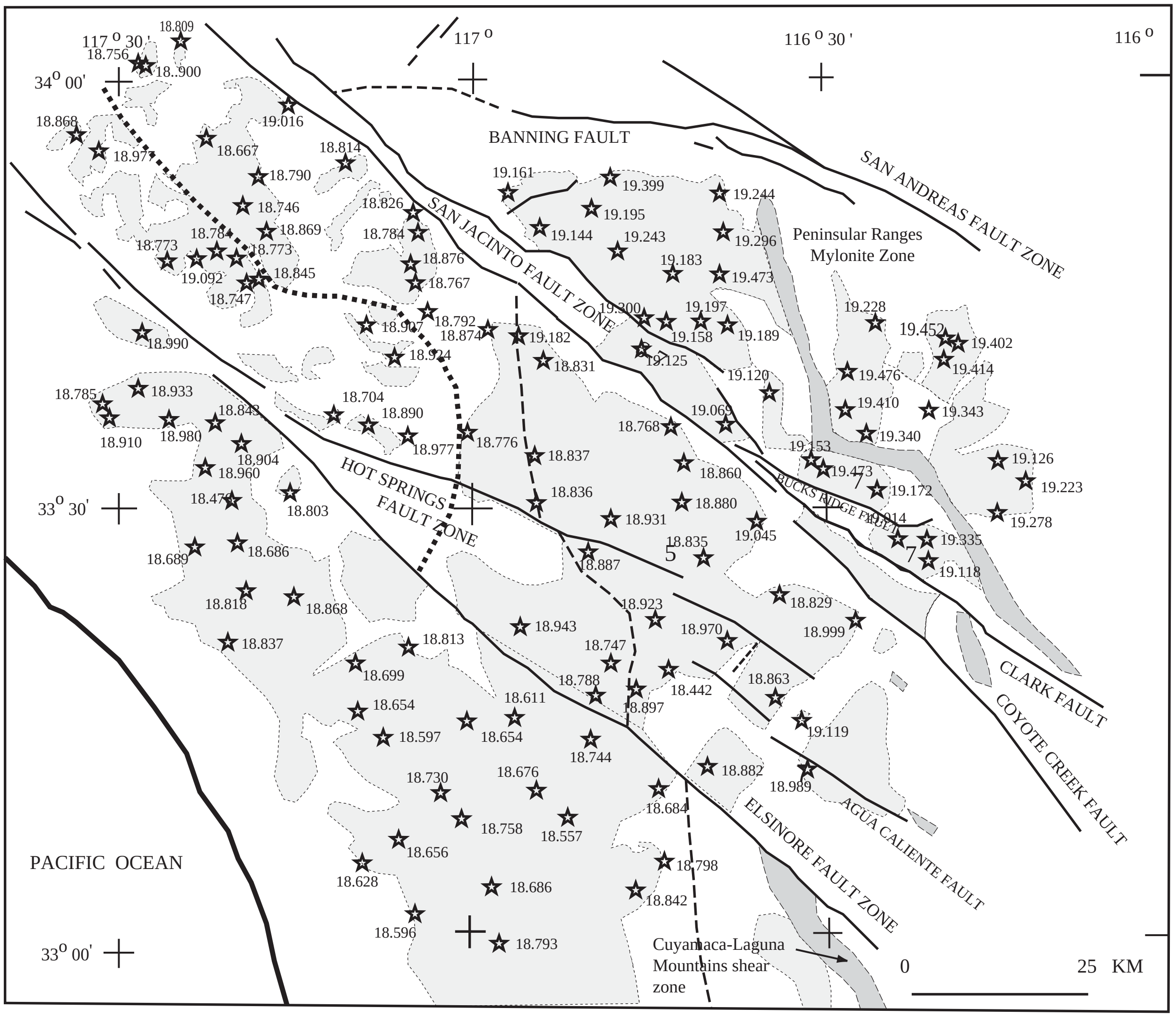

Figure 5. Specimen locations and initial $^{206}Pb/^{204}Pb$ values in the northern Peninsular Ranges batholith. The oxygen isotope step (Figure 4) is shown by the northerly trending dashed line and the tectonic boundary of Morton and Gray (2002) is shown by the heavy dotted line.

The San Jacinto block lies between the San Andreas and San Jacinto Fault zones (Figure 1). Rather than a single fault, the San Jacinto fault zone is defined by a number of segments (Sanders and Magistrale, 1997). With a few exceptions, Sri in plutons of the San Jacinto block are >0.706 and isotopic boundaries are very complex. The San Jacinto fault zone is more a diffuse boundary than an isopleth that separates plutons with Sri>0.706 from those with Sri<0.706. Hill and Silver (1988) and Hill and others (1986) reported results of detailed studies of Sri and oxygen isotopes, respectively, in the composite San Jacinto pluton and other plutons in the northern part of the block west of the Peninsular Ranges mylonite zone. They found Sri and ∂^{18}O in these plutons to range from 0.7058 to 0.7076 and from 9.0 to 10.6 permil, respectively. From our work, with the exception of those with Sri=0.705 between the Coyote Creek fault and Clark fault segments, Sri and ∂^{18}O of plutons in the whole block below the mylonite zone range from 0.706 to 0.708 and from 8.3 to 12.8 permil, respectively (Tables 2, 3, Figures 3, 4). Plutons above the mylonite zone have Sri greater than 0.707 and less than 0.709 and ∂^{18}O values that range from 8.3 permil to 9.1 permil (Figures 3, 4, 6).

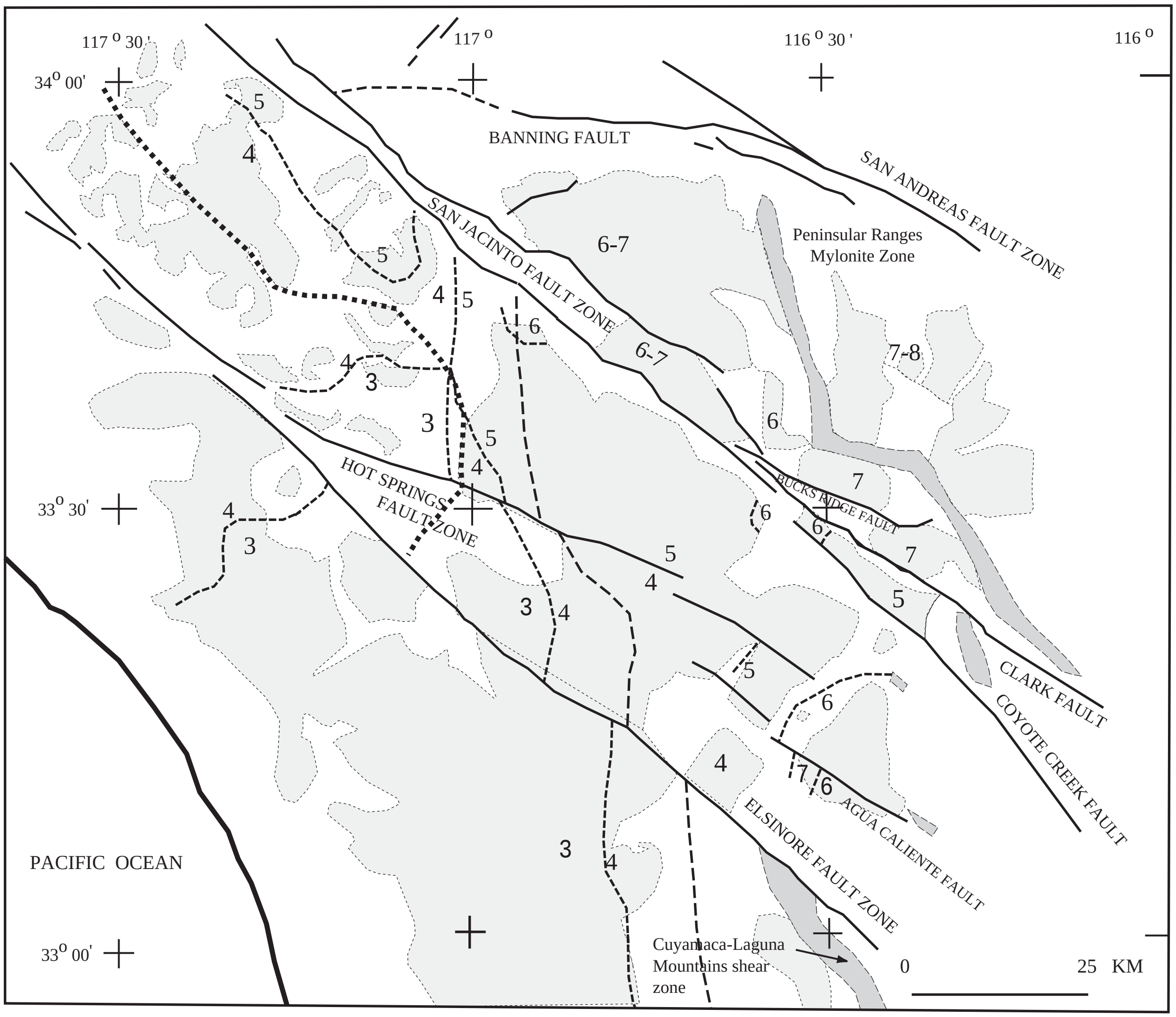

Figure 6. Sri isopleths (short-dashed lines) on the map of granitic rock exposures (gray) in the northern Peninsular ranges batholith are shown only for third place values of Sri. For example, the isopleths between 3 and 4 are 0.704 lines and between 4 and 5 are 0.705 lines. 0.704 lines separate plutons with Sri values of 0.7030-0.7039 from those with Sri values of 0.7040-0.7049. 0.705 lines separate plutons with Sri values of 0.7040-0.7049 from those with Sri values of 0.7050-0.7059. The location of the oxygen isotope step from Figure 4 (long-dashed lines) and the tectonic boundary of Morton and Gray (2002) heavy dotted line are also shown.

ISOTOPE VARIATIONS AND PLUTON SOURCE MATERIALS

Isotopic compositions of granitic plutons in the Northern Peninsular Ranges batholith are variable and a function of geographic position and not of rock composition. This requires that the isotopic variations observed are source related and are not due to processes like magmatic fractional crystallization or wall rock contamination.

A plot of Sri vs ∂^{18}O (Figure 7) for plutons in the northern Peninsular ranges batholith shows a west to east increase and a broad, generally positive correlation of both isotope ratios. Plutons in the Santa Ana and Perris blocks with Sri<0.704 and δ^{18}O< 9.0 permil probably were derived from tholeitic sources, whereas those with Sri ≥0.704 <0.706 and δ^{18}O < 9.0 permil probably were derived from more alkalic and silicic sources. Perris block plutons with Sri ≥0. 704 <0.706 and δ^{18}O ≥9.0 permil (EPRB) pose a source material problem, here, and in the entire EPRB (Taylor, 1986). Taylor concluded partial melting of eclogite-facies altered basaltic material mixed with a sedimentary component like the Franciscan formation can account for the strontium and oxygen isotopic characteristics of the magmas that formed these plutons. Our data are compatible with his conclusion. In the Perris block, the two specimens with Sri > 0.706 and δ^{18}O=12.3 permil are isotopically similar to San Jacinto block plutons below the mylonite zone. One isolated specimen (B406) may have an entirely sedimentary rock source (Sri=0.713, δ^{18}O=18 permil, Figure 7). Plutons in the San Jacinto block have Sri >0.705<0.709 and δ^{18}O >8.0<13.0 permil. Most of the data define a broad field that overlaps and forms a continuum with the EPRB Perris block data and indicates a similar source but with a larger proportion of sedimentary materials to account for the more radiogenic Sri and heavier δ^{18}O. However, eleven specimens plot away from the main array and cluster about Sri=0.708±0.0005 and δ^{18}O=8.5±0.5 permil (figure 7). All, but one of these specimens are from above (to the east of) the Peninsular Ranges mylonite zone and have a source that probably is crystalline continental lithosphere material.

Figure 8 shows δ^{18}O vs ^{206}Pb/^{204}Pb values that have a broad, generally positive correlation. In the Santa Ana block, the specimens with ∂^{18}O values <+6.0 permil probably interacted with hydrothermal meteoric water that lowered the characteristic unmodified granitic rock values of 6.0 to 9.0 permil. This alteration, however, did not noticeably change the lead isotopic values or the Sri values (Figure 7) for the specimens. The Perris block specimen with δ^{18}O=18.2 does not have a ^{206}Pb/ ^{204}Pb value noticeably different from other Perris block specimens, but does have an extraordinary Sri (Figure 7) that along with the heavy oxygen indicates a sedimentary rock source for this pluton. The Perris block specimen with the most primitive ^{206}Pb/^{204}Pb=18.44 is from a gabbro that indicates a source like that for WPRB plutons exists beneath the main source region for the EPRB plutons. In the Perris and Santa Ana blocks, most of the WPRB plutons have ^{206}Pb/^{204}Pb values from about 18.5 to 19.0 and δ^{18}O values from6.0 to 9.0 permil that are compatible with mafic igneous source materials. Those Perris block specimens with ^{206}Pb/^{204}Pb from about 18.8 to 19.0 but with δ^{18}O values >9.0 permil can have similar mafic igneous sources with additional sedimentary sources like Franciscan Formation. The two Perris block specimens with ^{206}Pb/^{204}Pb values >19.0 and δ^{18}O=12.3 permil have Sri>0.706 and are isotopically similar to San Jacinto block plutons east of the mylonite zone.

Samples from the San Jacinto block to the east of the Peninsular Ranges mylonite zone show a positive correlation of $^{206}Pb/^{204}Pb$ values from 19.0 to 19.5 with $\delta\ ^{18}O$ values from 9.0 to 12.8 permil (Figure 8). The data overlap with and extend the EPRB Perris block data to more radiogenic $^{206}Pb/^{204}Pb$ values but similar $\delta\ ^{18}O$ values. Together, the lead and oxygen isotopic compositions require a more radiogenic (continental?) sedimentary component in the source materials for the San Jacinto block plutons than for the Perris block plutons. Samples to the east

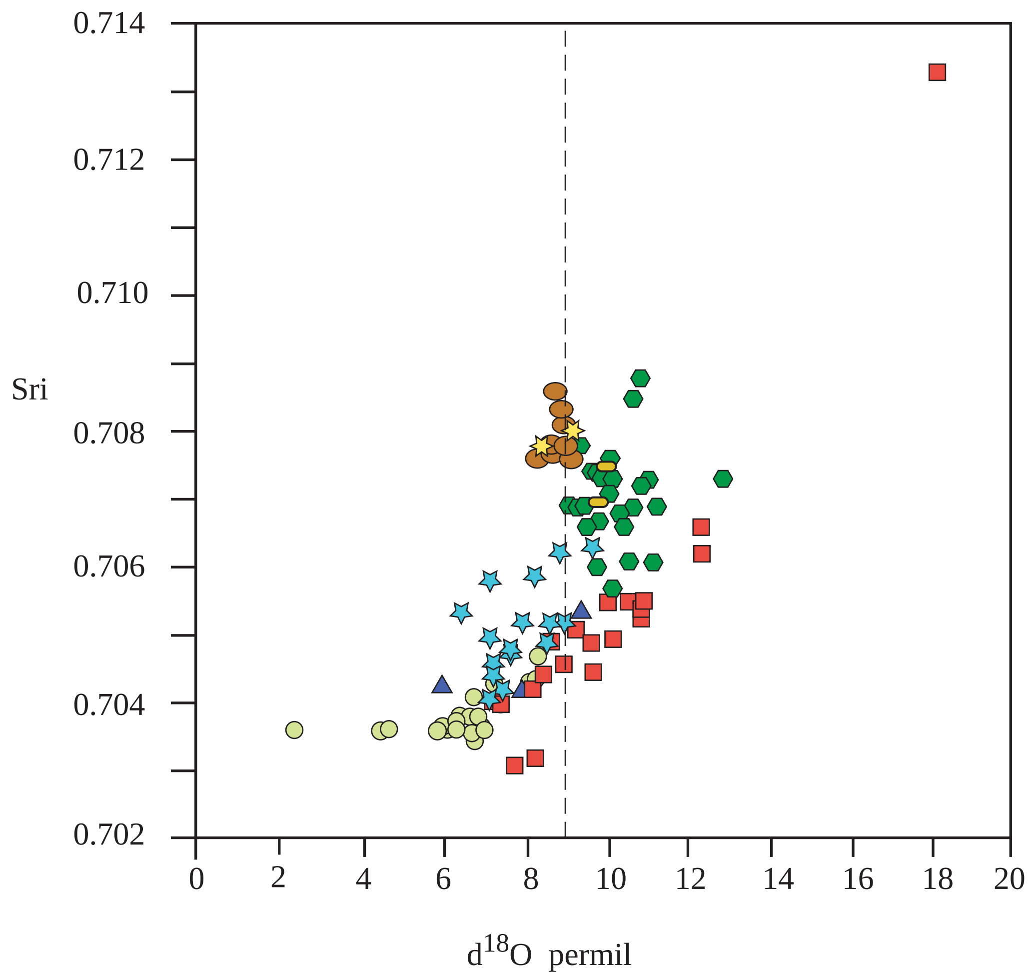

Figure 7. Plot showing Sri vs. $\delta^{18}O$ values for plutons in the northern Peninsular Ranges batholith. Symbols: circles, Santa Ana block; squares, Perris block; hexagons, San Jacinto block below the mylonite zone; ellipses, San Jacinto block above the mylonite zone. Symbols for samples from the zircon dating traverse of Premo and others (1997): triangles, Santa Ana block; five pointed stars, Perris block; ellipses, San Jacinto block below the mylonite zone; six pointed stars, San Jacinto block above the mylonite zone. The vertical dashed line marks $\delta\ ^{18}O$ = 9.0 permil and separates, samples from the eastern and western Peninsular Ranges batholith, respectively.

of the Peninsular Ranges mylonite zone have a comparable range of $^{206}Pb/^{204}Pb$ but lighter and more uniform oxygen isotopic values of 8.5±0.5 than specimens have to the west the mylonite. This, in combination with the strontium isotopic data for the same rocks is compatible with crystalline continental lithosphere material in the source for these rocks.

Figure 9 is a plot of Sri vs initial $^{206}Pb/^{204}Pb$ for northern Peninsular Ranges plutons. Data from all but four samples fall within three fields delineated by dashed lines: field A >0.702 <0.704, > 18.4<19.0; field B ≥0.704<0.706, >18.4<19.0; field C ≥0.706<0.709, >19.0<19.6 for Sri and initial $^{206}Pb/^{204}Pb$, respectively.

Both strontium and lead isotopes for specimens from the Santa Ana and Perris blocks in field A are compatible with a tholeiitic source material for these plutons. All but one sample are inside the 0.704 isopleth on Figure 6 and are in the WPRB. Gabbro sample B393 (Table 3) is in the Perris block in the EPRB.

Samples in field B are from are from the Santa Ana and Perris blocks and the data can be subdivided into two fields. One of these, with specimens from both blocks, has Sri ≥0.704<0.705 and $^{206}Pb/^{204}Pb$ >18.5<19.0, whereas the second has specimens only from the Perris block with Sri≥0.705<0.706 and $^{206}Pb/^{204}Pb$ >18.8<19.0. Most of the samples in the second field have $\delta^{18}O$ > 9.0 permil (Figure 8) that indicates a sedimentary rock component in their source materials.

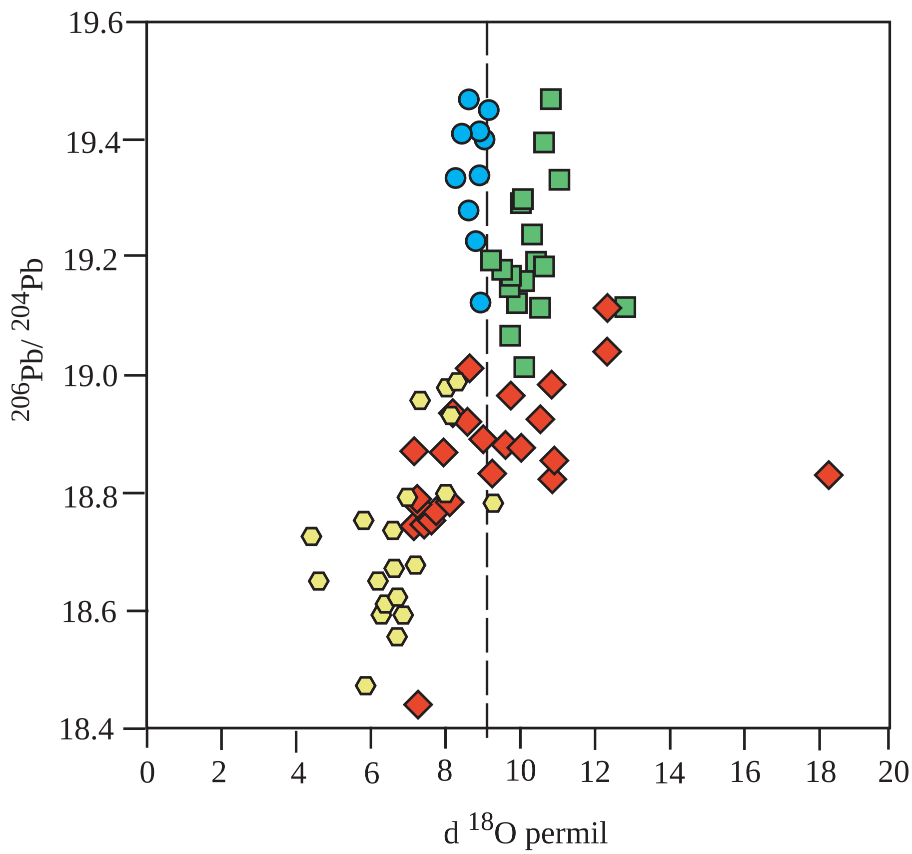

Figure 8. Initial $^{206}Pb/^{204}Pb$ vs $\delta^{18}O$ for plutons in the northern Peninsular Ranges batholith. Symbols: hexagons, Santa Ana block; diamonds, Perris block; squares, San Jacinto block below the shear zone; circles, San Jacinto block above the shear zone. The vertical dashed line at $\delta^{18}O$=9.0 permil separates, to the right and left, samples from the eastern and western Peninsular ranges batholith, respectively.

Except for three from the Perris block, all of the samples in field C are from the San Jacinto block. Sri (>0.706 <0.709), initial $^{206}Pb/^{204}Pb$ (>19.0<19.5), and $\delta^{18}O$ (>9.0<11.0 permil, Figures 7, 8) are positively correlated in plutons below the Peninsular Ranges Mylonite Zone.

These isotopic characteristics are compatible with sediments derived from a continental source in the source materials for the plutons. Samples above the mylonite have restricted ranges of initial $^{206}Pb/^{204}P$ (>19.1<19.5), Sri (0.708± 0.0005), and $\delta^{18}O$ (8.5±0.5) permil). All three isotopic characteristics are compatible with a crystalline continental lithosphere source for these plutons.

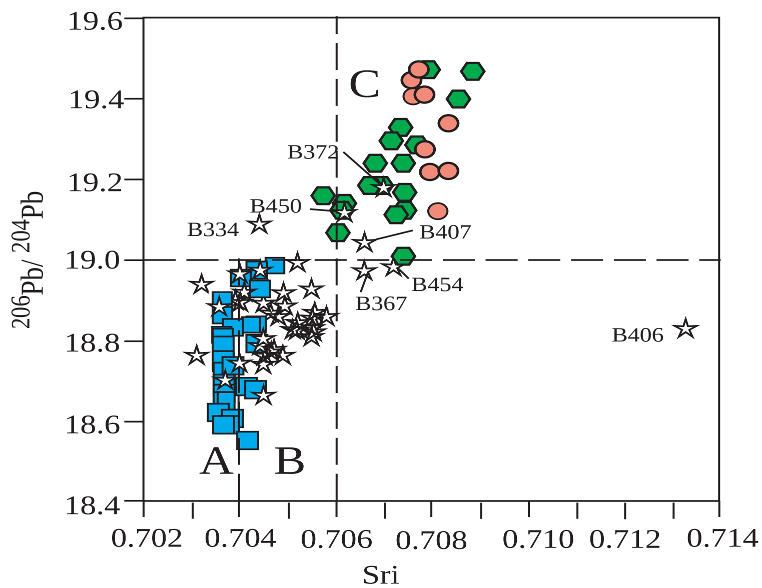

Figure 9. Initial $^{206}Pb/^{204}Pb$ vs Sri for plutons in the northern Peninsular Ranges batholith. Symbols: squares, Santa Ana block; stars, Perris block; hexagons, San Jacinto block below the shear zone; circles, San Jacinto block above the shear zone.

Perris block specimens B450, B454, B372, and B407 that plot in or just outside of field C, Figure 9, all have lead, strontium and oxygen isotopic values like plutons below the mylonite zone in the San Jacinto block. Specimen B407 in the Perris block and specimen B325 in the San Jacinto block, west and east of the Coyote Creek segment of the San Jacinto fault zone (Figure 2), respectively, have similar Rb and Sr concentrations and identical Sri. The geologic map compilation (Rogers, 1965) shows continuous granitic rock outcrops between these two specimens that are not separated by a fault. However, in the proximity of these two specimens, arcuate traces of shallowly dipping faults cut the granitic rocks and define the traces of both the Coyote Creek and Clark segments of the San Jacinto fault zone. Specimen B407 may be part of the San Jacinto block in thrust contact over the Perris block. Ramona Bowl pluton specimen B372 in the Perris block is just west of the Casa Loma segment of the San Jacinto fault zone. It too may be a San Jacinto block pluton on the Perris block side of the San Jacinto fault zone.

RUBIDIUM-STRONTIUM WHOLE-ROCK AGES

On his geologic map of the "Batholith and associated rocks of the Corona, Elsinore, and San Luis Rey quadrangles, southern California", Larsen (1948) assigned names to plutons based on outcrop characteristics such as grain-size, inclusion content, color, and relative abundances of different minerals. Several of these named units occur as discrete plutons over large areas of up to 250 square miles. Comparison of the locations of granitic rock samples collected by Baird and his colleagues to this map permits their assignment to these plutons. In the Santa Ana block, between 33º and 33º30´ N. Lat., all Rb-Sr whole-rock data from three of these named units, Bonsall Tonalite, Woodson Mountain Granodiorite, and Green Valley Tonalite were plotted on strontium evolution diagrams (Figures 10, 11, and 12, respectively). Rb-Sr whole-rock ages of 105.2±8.1 Ma, 123.7±5.6 Ma, and 117±14 Ma for the Bonsall Tonalite, Woodson Mountain Granodiorite, and Green Valley Tonalite, respectively, are derived by regression of these data (Ludwig, 1999). All units have a very primitive Sri=0.7037±0.0001.

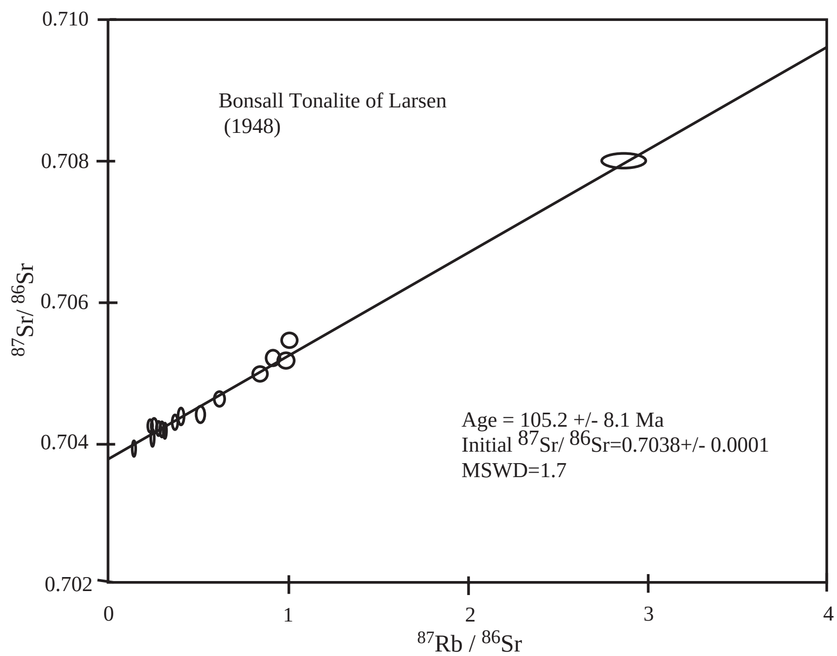

Figure 10. Rb-Sr whole-rock isochron plot for specimens of Bonsall Tonalite south of 33º30´ N. Lat. in the Santa Ana block (Figure 3).

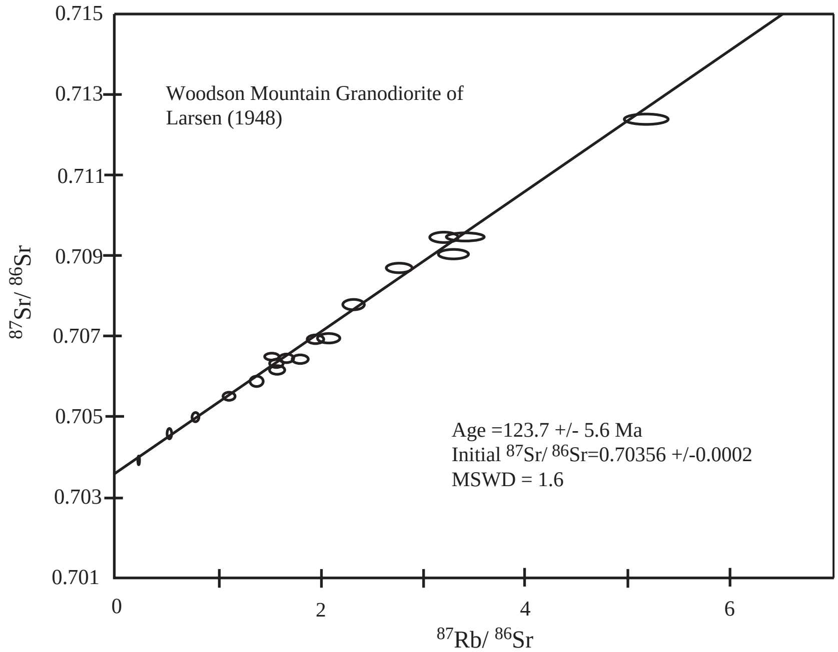

Figure 11. Rb-Sr whole-rock isochron plot for specimens of Woodson Mountain Granodiorite south of 33º30´ N. Lat. in the Santa Ana block (Figure 3).

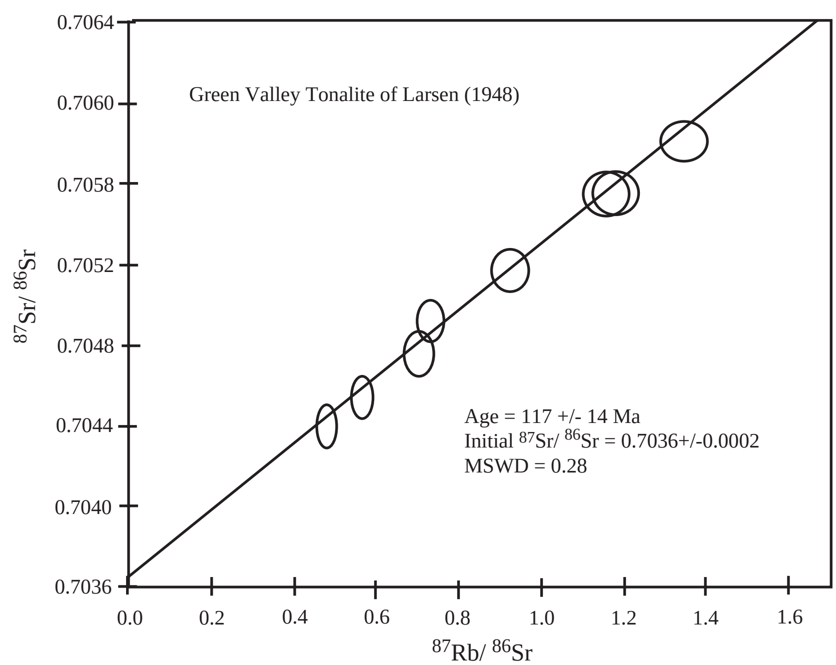

Figure 12. Rb-Sr whole-rock isochron plot for specimens of Green Valley Tonalite south of 33º30´ N. Lat. in the Santa Ana block (Figure 3).

Most of the northern part of the San Jacinto block, west of and beneath the Peninsular Ranges Mylonite Zone (Figure 2), is made up of the tonalitic rocks of the 94 Ma San Jacinto Intrusive Complex (Hill and others, 1986). These workers reported large variations in Sri from samples of the tonalites. Samples from this complex collected by Baird and his colleagues confirm this variation of Sri calculated for 94 m. y. (Table 2, Figure 3). Unlike many of the granitic rocks in the Santa Ana block, the extreme variation in Sri from the San Jacinto Intrusive Complex does not permit the use of Rb-Sr whole-rock data as a geochronometer for these rocks.

In the Perris block, exposed between the Elsinore and Hot Springs fault zones north of Lake Henshaw, nine adjacent samples (B401, B404, B410-416) of quartz diorite, granodiorite, and quartz monzonite have strontium isotopic data (Table 2) that yield a Rb-Sr whole-rock isochron age of 153±14 Ma, Sri=0.7040±0.0002 (Figure 13). However, plots of Sri at 100 Ma vs 1/Sr and Sri vs $\delta\,^{18}O$ for these specimens are linear with R^2 =0.83 and 0.94, respectively. These linear plots indicate that the isochron is a mixing line (Faure and others, 1974; Kistler and others 1986). However, some credibility is given to the apparent Late Jurassic age because it is similar to a multiple fraction, conventional U-Pb zircon age (156±12 Ma) for a gneiss in the Cuyamaca-Laguna Mountains shear zone (e.g. Figure3) south of the Elsinore fault zone (Walawender and others, 1991). Additional dating of plutons in this area by both U-Pb and Rb-Sr techniques are required to establish these ages with certainty.

North of 33º30´ N. Lat. in the northern Perris block, Larsen (1948) assigned the name Woodson Mountain Granodiorite to a large pluton called the Cajalco quartz monzonite by Dudley (1935). The Cajalco pluton is 108 Ma by U-Pb zircon dating (Premo and others, 1997) and 109±4 Ma by Rb-Sr whole rock dating (Figure 14).

A large pluton to the west of Val Verde in the Perris block, assigned to Bonsall tonalite by Larsen (1948), was renamed the Val Verde tonalite by Morton (1999). In contrast to the good agreement of ages by the two dating techniques for the Cajalco pluton, the U-Pb zircon date is 106 Ma (Premo and others, 1997) whereas the Rb-Sr whole-rock date is 129±18 Ma (Table 2, Figure 15). We accept the U-Pb zircon date as the correct age for this pluton. Even though the data that define the isochron for this body are analytically precise (MSWD=0.30), the $^{87}Rb/^{86}Sr$ values only range from about 0.3 to 1.14. A small increase of about 3 in the fourth place in measured $^{87}Sr/^{86}Sr$ for the most radiogenic sample could account for the older apparent age. Sri values for the Val Verde samples, calculated for an age of 106 Ma, range from 0.7045 to 0.7048 (Table 2). The calculated Sri=0.7048 is for the specimen with $^{87}Rb/^{86}Sr$=1.14.

The $^{87}Rb/^{86}Sr$ for the Cajalco pluton samples range from 0.049 to 5.5. Small variations in Sri for the most radiogenic specimens would not have a large effect on the slope of the isochron and the isochron age is the same as the U-Pb zircon age. In the few other plutons with both Rb-Sr whole-rock and U-Pb zircon dates sampled in this study, the ages agree for the Box Springs and Lakeview Mountains plutons but differ for the Wilson Valley pluton (Table 2).

Silver and others (1979) report U-Pb zircon ages that range from about 120 Ma to 105 Ma for 12 plutons in a traverse across the western Peninsular Ranges batholith south of 33º N. Lat. near the international border. Our Rb-Sr whole-rock ages for the Bonsall tonalite, Green Valley tonalite, and Woodson Mountain granodiorite in the western Peninsular ranges batholith to the north of their traverse and south of 33º30´ N. Lat. have the same range in age. This concordance of ages by the two methods suggests the plutons were emplaced between about 120 and 105 Ma.

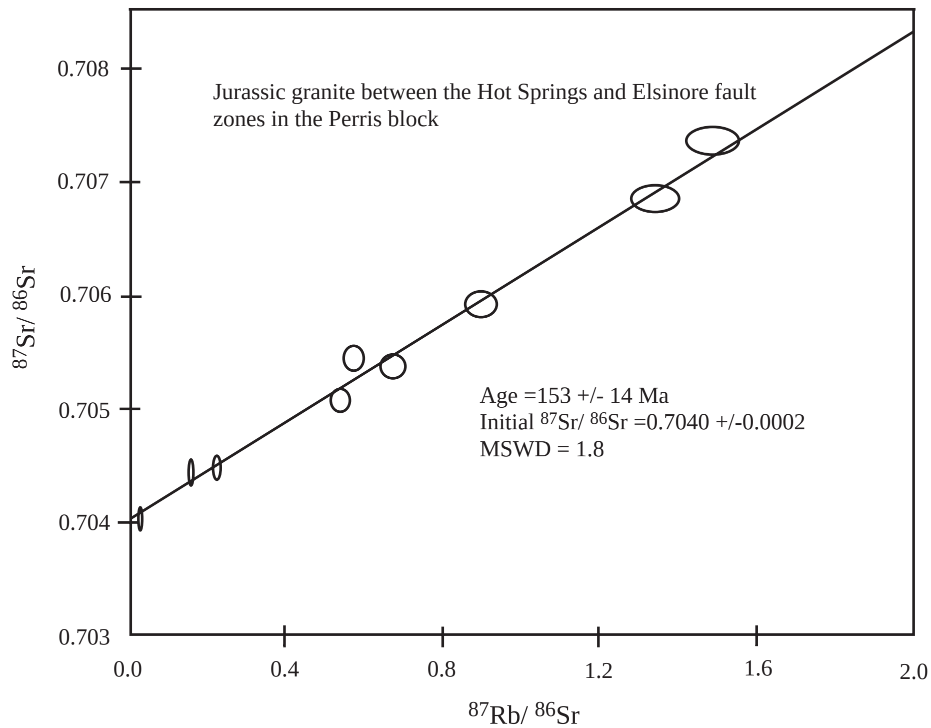

Figure 13. Rb-Sr isochron diagram for Late Jurassic (?) quartz diorites, granodiorites, and quartz monzonites exposed between the Hot Springs and Elsinore fault zones in the Perris block (Figure 3).

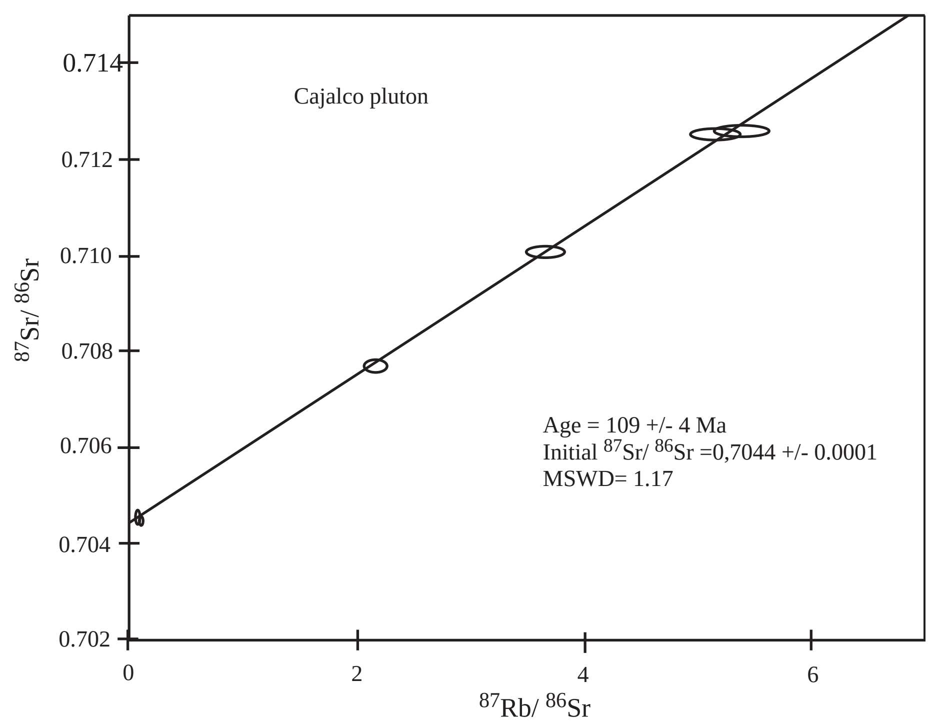

Figure 14. Rb-Sr whole-rock isochron plot for the Cajalco pluton exposed in the Perris block (Figure 3).

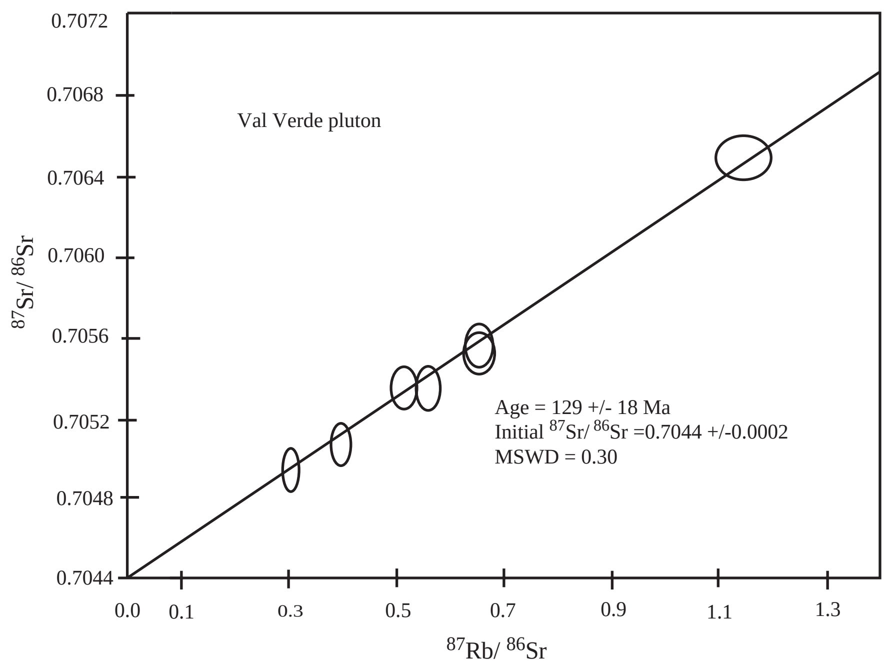

Figure 15. Rb-Sr isochron diagram for the Val Verde pluton exposed in the Perris block (Figure 3).

SUMMARY AND DISCUSSION

The primary purpose of this report is to make available the considerable isotopic data determined for granitic rock samples collected by Baird and others (1979) from the northern Peninsular Ranges batholith in the laboratories of the USGS in Menlo Park, California (Tables 1, 2, 3). We point out some interesting features, some relatively new and others possibly at odds with conclusions based on other studies in the batholith, that are revealed by these data.

The data of this report permit a comparison of Rb-Sr whole-rock ages with U-Pb zircon ages for some of the plutons mapped in the northern Peninsular Ranges batholith. The data confirm the observation that dating by multiple techniques on the same samples is the most reliable way to determine the meaning (emplacement, reset, contaminated, inherited) of an age for a Mesozoic pluton in a complex batholith terrane (e.g. Kistler and Wooden, 1994; Kistler and Champion, 2001).

In the Santa Ana block south of latitude 33°30', plutons called Woodson Mountain granodiorite , Green Valley tonalite, and Bonsall tonalite by Larsen (1948) have Rb-Sr whole-rock ages that range from about 125 Ma to 105 Ma that are the same as ages determined by U-Pb zircon dating (Silver and others, 1979) in plutons immediately south of our area of investigation. In this case, the concordance of ages by both techniques indicates they approximate emplacement ages. In contrast, samples of the Val Verde pluton in the Perris block have apparent ages of 129 Ma by Rb-Sr whole-rock dating and 106 Ma by U-Pb zircon dating. In this case, probably the "Rb-Sr isochron" is a mixing line determined by specimens that had different Sri at the time of their formation and the U-Pb zircon date approximates the pluton's emplacement time.

A group of samples in the Perris block yield a Rb-Sr whole-rock isochron age of 153 Ma.

This apparent age, old for the Peninsular Ranges batholith, is similar to a 156 Ma U-Pb zircon date for a nearby pluton (Walawender and others, 1991). The ages of zircon fractions used in the age determination are discordant due to inheritance of older zircons. The inheritance, plus possible lead loss from the zircons because of thermal events subsequent to emplacement of the pluton does not permit a simple interpretation of the age. Samples of the rocks that define the Jurassic "isochron" have linear correlations of 1/Sr and $\delta\ ^{18}O$ vs Sri that suggest a mixing line. However, additional support for both of these ages is given by Johnson and others (1999) in a mapping and SHRIMP U-Pb dating study in the Peninsular Ranges batholith in Baja California. Their data indicate that some plutons of the eastern Peninsular Ranges batholith represent a continental-margin arc initiated at least 140 m.y. ago. Additional dating and mapping in the area of our apparently Jurassic plutons in the northern Peninsular Ranges batholith is required to verify or deny the validity of the dates as emplacement ages.

The determination of Sri for all of the plutons from the Baird collection permits us to construct Sri isopleths on a map of the batholith to within approximately ±3 km (Figure 6). Because of this, some details are revealed along the well documented, but diffuse, geophysical and geological boundary between the EPRB and WPRB.

A Sri=0.704 isopleth trends north in the Santa Ana and Perris blocks and marks the radiogenic isotopic boundary between the EPRB and WPRB. Here the Sri=0.704 isopleth is parallel to and within the geophysical and geologic boundary. It is parallel to and 10 km to the west of the boundary between plutons with $\delta^{18}O < 9.0$ and ≥ 9.0 step (Figures 4, 6) that is also in the main PRB boundary zone. However, in the middle of the Perris block, the Sri=0.704 isopleth diverges to the west and is truncated at the Elsinore fault zone. Another westerly trending Sri=0.704 isopleth, also truncated by the Elsinore fault zone, is in the northern part of the Santa Ana block. By observation (Figure 6), these west-trending Sri=0.704 isopleths are offset about 17 km in a left lateral sense across the Elsinore fault zone. The north-trending Sri=0.704 isopleths are offset about 10 km and 7 km in a left lateral sense across the Elsinore and Hot Springs fault zones, respectively. Restoration of left lateral offsets of the west-trending Sri=0.704 isopleths across the Elsinore fault zone and north-trending Sri=0.704 isopleth across the Hot Springs and Elsinore fault zones suggests the west-trending Sri=0.704 isopleth images an old transform crustal boundary fault in the WPRB.

In the Perris block there are three plutons with strontium, lead, and oxygen isotopic values that are like those in plutons below the Peninsular Ranges mylonite zone in the San Jacinto block (Figures 7, 8, 9). These three plutons and plutons in the San Jacinto block east of the San Jacinto fault zone all have Sri greater than 0.706, with a few isolated exceptions, including a Sri=0.705 pluton between the Coyote Creek and Clark fault segments (figure 6). The San Jacinto fault zone exclusive of the Coyote Creek fault segment can be considered a Sri≥0.706 isopleth that marks a major discontinuity in the isotopic composition of source materials of plutons in the northern Peninsular Ranges batholith. This observation is compatible with the model for the petrochemical nature of source materials of batholithic rocks of southern California (Baird and Miesch, 1984) that identified a discontinuity in source compositions approximately coincident with the San Jacinto fault zone. They interpreted the fault as the western limit of significant contributions of sialic continental materials to the batholithic rocks.

In the area of our study, the strontium and oxygen isotopic characteristics of the plutons in the EPRB are the same as those of plutons intruded into Panthalassan lithosphere (Kistler, 1990) in the Sierra Nevada. This lithosphere is in tectonic contact with North American lithosphere in the southern Sierra Nevada. Plutons intruded into Panthalassan lithosphere are characterized by $\delta^{18}O$ values consistently greater than +9 permil in those with Sri>0.706 and often greater than +9 permil in those with Sri<0.706. The isotopic, especially $\delta^{18}O$> 9.0 permil, and chemical characteristics of the plutons in Panthalassa indicate a significant sedimentary rock component in the sources of their parent magmas. Kistler (1990) used these characteristics and others to indicate that, by itself, Sri greater than 0.706 in plutons does not characterize the basement beneath the plutons as crystalline Precambrian sialic crust, as suggested by Kistler and Peterman (1973). This is supported by the absence of direct remnants of Proterozoic sialic crystalline basement found in exposures of mid-crustal levels of the batholith (8kbar) in Panthalassan lithosphere in the southern Sierra Nevada (Sams, 1986; Saleeby and others, 1987). In the area of our present study, $\delta^{18}O$ >9.0 per mil and petrochemical source models (Baird and Miesch, 1984) indicate that in the EPRB the increase in Sri from 0.704 to 0.708 probably only represents a change from mafic (Franciscan) to felsic (continental) derived sediments. This change is sediment composition is marked by the most radiogenic plutons (Sri>0.706) like the few in the Perris block and all those west of the shear zone in the San Jacinto block.

Hill and others (1986) and Taylor (1986) proposed a third source component to account for those plutons in the San Jacinto block below the mylonite zone with $\delta^{18}O$ >+9.0 <+12.8 per mil and Sri >0.7057<0.708. On the Sri vs $\delta^{18}O$ plot these samples trend off of the main trend of Taylor and Silver (1978) toward a modeled source with Sri~0.710 and $\delta^{18}O$~+6 permil (Hill and others, 1986). They suggest rock with these isotopic characteristics could be old (>1Ga) material of basaltic composition. However, most of the data that trend toward the old basaltic end member are from rocks east of the Peninsular Ranges mylonite zone and are probably exotic to the Peninsular Ranges batholith and not relevant to models of source materials of the batholith.

Right lateral offset of 10-15 km along the main trace of the Elsinore fault zone is indicated by displaced contours of biotite K-Ar cooling ages of plutons on either side of the fault (Morton and Miller, 1987, inset figure in Morton and Gray, 2002). This is a contradiction to the 17 km of left lateral displacement along the fault indicated by offset of the west-trending Sri=0.704 isopleth discussed above. A possible resolution of the apparently conflicting directions of displacement along the Elsinore fault follows.

In regional studies of granitic rock terranes, undisturbed isotopic boundaries (e.g., Sri or $\delta^{18}O$ isopleths) represent the lines of intersections of *steeply dipping* surfaces such as pluton contacts with the surface exposure. Although these may be tilted or rotated during subsequent deformation, unless translated laterally by "thin-skinned" tectonic processes (e.g., detachment faulting), isotopic boundaries commonly occur nearly vertically above the differences in igneous source regions they represent. Conversely, undisturbed regional cooling-age contours represent the intersections of originally *shallow-dipping*, commonly isothermal surfaces, sub-parallel to the Earth's surface (in this case, the time rocks cooled to the closure temperature of biotite for argon). The critical age contour (108 Ma) used to determine the right lateral separation across the Elsinore fault zone (Morton and Miller, 1987) is adjacent and parallel to the fault for about 55 km, dipping shallowly southwest in the Perris block north and east of the fault. Within the Santa Ana block, southwest of the elsinore, the 108 Ma age contour dips more steeply west and strikes into the fault trace at an angle of forty degrees (Morton and Gray, 2002). Clearly, the originally sub-horizontal isohermal surface represented by the 108 Ma contour has been warped, tilted, and possibly rotated during much more recent deformation, some of which may be due to faulting along the Elsinore fault itself. Rotational differential uplift and erosion of the Santa Ana block along the fault occurring at any time in the 108 Ma following cooling could produce many non-unique highs and lows in the 108 Ma surface whose present configuration could result in the apparent 10-15 km separation across the fault. Some of this uplift and deformation could have occurred during left lateral displacement, matching anywhere along the 55km exposure in the Perris block north of the fault. The steeply dipping surfaces represented by the Sri=0.704 and $\delta^{18}O$ isopleths would be much less affected by differential uplift and would require regional rotation to produce significant changes in their trends. Their offsets across the Elsinore fault would approximate the amount of lateral displacement.

References cited

Baird, A.K., Baird, K.W., and Welday, E.E., 1979, Batholithic rocks of the northern Peninsular and Transverse Ranges, southern California: chemical composition and variation *in* Abbott, P.L. and Todd, V.R., eds., Mesozoic Crystalline Rocks: Peninsular Ranges batholith and pegmatites, Point Sal ophiolite: Department of Geological Sciences, San Diego State University, San Diego, CA, Guidebook for Geological Society of America Annual Meeting, p. 111-132.

Baird, A. K., and Miesch, A. T., 1984, Batholithic rocks of southern California- A model for the petrochemical nature of their source materials: U.S. Geological Survey Professional Paper 1284, 42 p.

Bateman, P.C. Clark, L.D., Huber, N.K., Moore, J.G., and Rinehart, C.D., 1963, The Sierra Nevada batholith- a synthesis of recent work across the central part: U.S. Geological Survey Professional Paper 414-D, 46p.

Bothwick, J. and Harmon, 1982, A note regarding ClF_3 as an alternative to BrF_5 for oxygen isotope analyses: Geochimica Cosmochimica Acta, v. 46, p.1665-1668.

Clayton, R.N. and Mayeda, T.K., 1963, The use of bromine pentafluoride in the extraction of oxygen from oxides and silicates for isotopic analysis: Geochimica Cosmochimica Acta, v.27, p.43-52.

Diamond, J.L., Knaack, C.M., Gastil, R.G., Erskine, B.G., Walawender, M.J., Marshall, M., and Cameron, G.J., 1985, The magnetite-ilmenite line in the Peninsular Ranges of southern and Baja California, U.S.A. and Mexico: Geological society of America Abstracts with Programs, v. 17, p.351.

Dudley, P.H., 1935, Geology of a portion of the Perris block, Southern California: California Journal of Mines and Geology, Quarterly chapter of the State Mineralogist, Report 31, no. 4, October.

Early, T.O., and Silver, L.T., 1973, Rb-Sr isotopic systematics in the Peninsular Ranges batholith of southern and Baja California: EOS, Transactions of the American Geophysical Union, vol.54, p.494.

Engel, A.E.J., and Schultejann, P.A., 1984, Late Mesozoic and Cenozoic tectonis history of south central California: Tectonics, vol. 3, no.6, p. 659-675.

Faure, G., Bowman, J.R., Elliott, D.H., and Jones, L.M., 1974, Strontium isotopic copositionn and petrogenesis of the Kirkpatrick basalt, Queen Alexandra Range, Antarctica: Contributions to Mineralogy and Petrology, v. 48, p. 153-169.

Gastil, R.G., 1975, Plutonic zones in the Peninsular Ranges of southern California and northern Baja California: Geology, v.3, p. 361-363.

Gastil, G., 1990, The boundary between the magnetite-series and ilmenite-series granitic rocks in Peninsular California: University Museum, University of Tokyo, Nature and culture, No.2, p. 91-100.

Gromet, L.P., and Silver, L.T., 1987, REE variations across the Peninsular Ranges batholith: Implications for batholith petrogenesis and crustal growth in magmatic arcs: Journal of Petrology, v. 28, no.1 , p.75-125.

Hill, R.I. and Silver, L.T., 1988, San Jacinto intrusive complex, 3, Constraints on crustal magma chamber processes from strontium isotope heterogeneity: Journal of Geophysical Research, vol. 93, no. B9, p. 10373-10388.

Hill, R. I., Silver, L. T., and Taylor, H. P., 1986, Coupled Sr-O isotope variations as an indicator of source heterogeneity for the northern Peninsular Ranges batholith: Contributions to Mineralogy and Petrology, v. 92, p.351-361.

Jachens, R.C., Todd, V.R., Morton, D.M., and Griscom, A., 1991, Constraints on the structural evolution of the Peninsular Ranges batholith, California, from a new aeromagnetic map: Seismological Research Letters, v. 62, no. 1, p.44.

Johnson, S.E., Tate, M.C., and Fanning, C.M., 1999, New geologic mapping and SHRIMP U-Pb zircon data in the Peninsular Ranges batholith, Baja California, Mexico: Evidence for a suture: Geology, v. 27,no. 8, p. 743-746.

Kistler, R.W., 1990, Two different lithosphere types in the Sierra Nevada California: *in* Anderson, J.L., ed., The nature and origin of cordilleran magmatism: Geological society of America Memoir 174, p.271-281.

Kistler, R.W., Chappell, B.W., Peck, D.L., and Bateman, P.C., 1986, Isotopic variation in the Tuolumne intrusive suite, central Sierra Nevada, California: Contributions to Mineralogy and Petrology, v. 94, p.205-220.

Kistler, R.W., and Champion, D.E., 2001, Rb-Sr whole-rock and Mineral ages, K-AR, $^{40}Ar/^{39}Ar$, and U-Pb mineral ages, and strontium, lead neodymium, and oxygen isotopic compositions for granitic roks from the Salinian composite terrane, California: US Geological Survey Open-File Report, OF 01-453, 83 p.

Kistler, R.W., and Wooden, J.L., 1994, Interpretation of U/Pb ages of zircons from Mesozoic plutons in the Salinian block, California: *in* Abstracts of the Eight International Conference on Geochronology, Cosmochronology and Isotope geology, Lanphere, M.A., Dalrymple, G.B., and Turrin, B.D., eds., U.S. Geological survey Circular 1107, p. 173.

Kistler, R.W., and Morton, D. M., 1994, Sr, Rb, Sri variation and whole-rock Rb-Sr ages of plutons in the northern Peninsular Ranges batholith, southern California: Geological Society of America Abstracts with Programs, v. 26. no.2, p.82.

Kistler, R.W., and Peterman Z.E., 1973, Variations in Sr, Rb, K, Na and initial $^{87}Sr/^{86}Sr$ in Mesozoic granitic rocks and intruded wall rocks in central California: Geological Society of America Bulletin, v. 84, p.3489-3512.

Kistler, R.W., Peterman, Z.E., Ross, D.C., and Gottfried, D., 1973, Strontium isotopes and the San Andreas fault, *in* Kovach, R. L., and Nur, A. eds., Conference on the tectonic problems of the San Andreas fault system, Proceedings: Stanford University Publications, Geological Sciences, v. 13, p. 339-347.

Larsen E. S., Jr., 1948, Batholith and associated rocks of the Corona, Elsinore, and San Luis Rey quadrangles, southern California: Geological Society of America Memoir 29, 182 P.

Lewis, J.L., Day, S.M., Magistrale, H., Eakins, J., and Vernon, F., 2000, Regional crustal thickness variations of the Peninsular Ranges, southern California: Geology, v., 28, no. 4, p, 303-306.

Lichte, F.E., 1994, Determination of minor and trace elemental signatures in the southern California batholith by laser ablation inductively coupled plasma mass spectrometry: Geological Society of America Abstracts with Programs, v.26, no. 2, p.66.

Ludwig, K.R., 1999, User's Manual for Isoplot/Ex, version 2.05: Berkeley Geochronology Center Special Publication no. 1a, 48p.

Magistrale, H. and Sanders, C., 1995, P-wave image of the Peninsular Ranges batholith, southern California: Geophysical Research Letters, v. 22, no. 18, p.2549-2552.

Merriam, R.H., 1941, A southern California ring dike, American Journal of Science, v. 239, p. 365-371.

Morton, D.M., 1999, Santa Ana 60′ quadrangle, southern California, version 1, U.S. Geoligical Survey Open-File Report 99-172 1:100,000

Morton, D.M., and Gray,C.H. Jr., 2002, Geologic map of the Corona North 7.5' quadrangle, Riverside and San Bernardino Counties, California: U.S. Geological Survey Open-File Report 02-22, scale 1:24,000.

Morton, D.M., and Kistler, R.W., 1997, Sri variation in the Peninsular Ranges batholith: Geological Society of America Abstracts with Programs, v.29, no.6, p. A-69.

Morton, D.M., and Miller, F.K., 1987, K/Ar apparent ages of plutonic rocks from the northern part of the Peninsular Ranges batholith, southern California: Geological Society of America Abstracts with Programs (Cordilleran section), v. 19, p.435.

Oliver, H.W., 1980, Peninsular Ranges, *in* Oliver, H.W., ed., Interpretation of the gravity map of California and its continental margin, California Division of Mines and Geology Bulletin 205, p.17-19.

Premo, W. R., Morton, D. M., Snee, L. W., Fanning. C. M., 1997, Isotopic ages and associated cooling histories for selected samples from the northern Peninsular Range batholith, S. California: Geological Society of America Abstracts with Programs, v. 29, no. 5, p. 57.

Roberts, C.W., Jachens, R.C., and Oliver, H.W., 1990, Isostatic residual gravity map of California and offshore southern California: Map No. 7, California geologic data map series, scale 1:750,000.

Rogers, T. H., 1965, compiler, Santa Ana Sheet: Geologic map of California, O. P. Jenkins edition, scale 1:250,000.

Saleeby, J.B., Sams, D.B., and Kistler, R. W., 1987, U/Pb zircon, strontium and oxygen isotopic and geochronological study of the southernmost Sierra Nevada batholith, California: Journal of Geophysical Research, v. 92, no. b10, p.10443-10466.

Sams, D.B., 1986, U/Pb geochronology, petrology, and structural geology of the crystalline rocks of the southernmost Sierra Nevada and Tehachapi Mountains, Kern County, California (PhD. Thesis): Pasadena, California Institute of Technology, 315 P.

Sanders, C.O., and Magistrale, H. 1997, Segmentation of the northern San Jacinto fault zone, southern California: Journal of Geophysical Research, v. 102, p.27453-27467.

Silver, L.T., Taylor, H.P. Jr., and Chappell, B.W., 1979, Some petrological, geochemical, and geochronological observations of the Peninsular Ranges batholith near the International border of the U.S.A. and Mexico *in*, Abbott, P.L, Todd, V.R. eds. Mesozoic Crystalline Rocks, Geological Society of America Annual Meeting Guidebook. P. 83-110.

Simpson, Carol, 1984, Borrego Springs-Santa Rosa mylonite zone: A Late cretaceous west-directed thrust in southern California: Geology, v. 12, p. 8-11.

Steiger, R.H., and Jager, E., 1977, Subcommission on geochronology: Convention on the use of decay constants in geo-and cosmochronology: Earth and Planetary Sciences Letters, v. 36, p.359-362.

Taylor, H.P. Jr, 1986, Igneous rocks II. Isotopic case studies of circumpacific magmatism *in* Valley, J.W., Taylor, H.P. Jr., O'Neil, J.R., eds., Stable isotopes in high temperature geological processes, Reviews in Mineralogy, v. 16, p.273-318.

Taylor, H.P. Jr., and Silver, L.T., 1978, Oxygen isotope relationships in plutonic igneous rocks of the Peninsular Ranges batholith, southern and Baja California: *in* Zartman, R.E., ed. Short Papers of 4th International Conference on Geochronology, Cosmochronology, Isotope Geology: U.S. Geological Survey Open-File Report 78-701, p.423-426.

Todd, V.R., and Shaw, S.E., 1985, S-type granitoids and an I-S line in the Peninsular Ranges batholith, southern California: Geology, v. 13, p.231-133.

Walawender, M.J., Girty, G.H., Lombardi, M.R., Kimbrough, D., Girty, M.S., and Anderson, C., 1991, A synthesis of recent work in the Peninsular Ranges batholith: in Geologic Excursions in southern California and Mexico, Walawender, M.J., and Hanan, B.B. eds., Guidebook for the 1991 Annual Meeting Geological of America: p.297-312.

Wooden, J.L., Kistler, R.W., Morton, D.M., and Lichte, F.E., 1994, A Pb, Sr and isotopic transect across the northern Peninsular Ranges batholith, southern California: EOS, Transactions of the American Geophysical Union, v.75, no. 44, p. 701.

Table 1. Samples, latitude and longitude, specific gravity and rock type of northern Peninsular Ranges granitic rocks

Sample	W. Longitude	N. Latitude	Specific gravity (g/cc)	Rock type
B223	-116.9377	33.8683	2.72	granodiorite
B224	-116.8986	33.8875	2.66	quartz monzonite
B225	-116.8635	33.8868	2.70	granodiorite
B226	-116.8311	33.8868	2.74	granodioritee
B227	-116.4034	33.6424	2.76	granodiorite
B228	-116.8964	33.8580	2.70	granodiorite
B229	-116.8975	33.8276	2.73	granodiorite
B230	-116.8592	33.8381	2.71	granodiorite
B231	-116.8282	33.8550	2.71	granodiorite
B232	-116.7978	33.8883	2.75	granodiorite
B233	-116.7614	33.8892	2.75	granodiorite
B234	-116.7953	33.8592	2.73	granodiorite
B236	-116.8503	33.8310	2.71	granodiorite
B237	-116.8613	33.7986	2.72	granodiorite
B238	-116.8260	33.7996	2.70	granodiorite
B239	-116.8254	33.7754	2.72	granodiorite
B240	-116.7947	33.8035	2.70	granodiorite
B241	-116.7945	33.8290	2.71	granodiorite
B242	-116.7612	33.8606	2.72	granodiorite
B243	-116.7241	33.8624	2.74	granodiorite
B244	-116.6886	33.8631	2.76	granodiorite
B245	-116.6518	33.8731	2.73	granodiorite
B246	-116.7568	33.8318	2.69	granodiorite
B247	-116.7216	33.8335	2.72	granodiorite
B248	-116.7568	33.8025	2.69	granodiorite
B249	-116.7915	33.7742	2.71	granodiorite
B250	-116.7857	33.7456	2.70	granodiorite
B251	-116.7607	33.7705	2.76	granodiorite
B252	-116.7210	33.8051	2.71	granodiorite
B253	-116.6486	33.8224	2.75	granodiorite
B254	-116.6891	33.8053	2.72	granodiorite
B255	-116.7224	33.7726	2.65	quartz monzonite
B256	-116.7526	33.7443	2.73	quartz diorite
B257	-116.7530	33.7245	2.73	granodiorite
B258	-116.7186	33.7190	2.73	granodiorite
B259	-116.6838	33.7464	2.66	quartz monzonite
B260	-116.6804	33.7709	2.74	granodiorite
B261	-116.6513	33.8036	2.72	granodiorite
B262	-116.5663	33.7796	2.70	granodiorite
B263	-116.6133	33.7799	2.72	granodiorite
B264	-116.6503	33.7782	2.68	quartz monzonite
B265	-116.6805	33.7200	2.77	granodiorite
B266	-116.6463	33.7207	2.63	quartz monzonite
B267	-116.6140	33.6902	2.62	quartz monzonite
B268	-116.6487	33.6905	2.70	granodiorite
B269	-116.6810	33.6881	2.77	granodiorite
B270	-116.5782	33.6345	2.67	quartz monzonite
B271	-116.5797	33.6056	2.65	quartz monzonite
B272	-116.5794	33.5765	2.70	granodiorite
B273	-116.5381	33.5772	2.75	granodiorite
B274	-116.5373	33.6295	2.75	granodiorite

Table 1. Samples, latitude and longitude, specific gravity and rock type of northern Peninsular Ranges granitic rocks

Sample	W. Longitude	N. Latitude	Specific gravity (g/cc)	Rock type
B275	-116.5062	33.6360	2.70	granodiorite
B276	-116.5093	33.6079	2.73	granodiorite
B277	-116.5064	33.5517	2.76	granodiorite
B278	-116.4679	33.5514	2.74	granodiorite
B279	-116.4662	33.5216	2.70	granodiorite
B280	-116.4313	33.5221	2.71	granodiorite
B281	-116.4301	33.4962	2.71	granodiorite
B282	-116.3973	33.5539	2.65	quartz monzonite
B283	-116.3660	33.5557	2.73	quartz monzonite
B284	-116.3333	33.5635	2.71	quartz monzonite
B285	-116.2939	33.5579	2.73	granodiorite
B286	-116.3298	33.5296	2.79	granodiorite
B287	-116.2901	33.5331	2.71	granodiorite
B288	-116.2614	33.5032	2.76	granodiorite
B289	-116.2270	33.5045	2.70	granodiorite
B290	-116.2295	33.5327	2.74	granodiorite
B291	-116.2256	33.5584	2.70	granodiorite
B292	-116.2628	33.5564	2.71	granodiorite
B293	-116.2613	33.5320	2.69	granodiorite
B294	-116.2646	33.6172	2.71	granodiorite
B295	-116.2981	33.6120	2.78	granodiorite
B297	-116.3321	33.6995	2.75	granodiorite
B298	-116.3300	33.6697	2.76	granodiorite
B299	-116.3316	33.6400	2.73	granodiorite
B300	-116.3647	33.6132	2.77	granodiorite
B301	-116.3770	33.6709	2.75	granodiorite
B302	-116.4350	33.7221	2.75	granodiorite
B303	-116.4672	33.7236	2.71	granodiorite
B304	-116.4717	33.6929	2.79	granodiorite
B305	-116.4341	33.6924	2.78	granodiorite
B306	-116.4666	33.6676	2.75	granodiorite
B307	-116.4342	33.6708	2.75	granodiorite
B308	-116.4364	33.6406	2.78	granodiorite
B309	-116.4698	33.6387	2.71	granodiorite
B310	-116.4736	33.6114	2.77	granodiorite
B311	-116.4342	33.6121	2.76	granodiorite
B312	-116.3985	33.4646	2.64	quartz monzonite
B313	-116.3613	33.4427	2.65	quartz monzonite
B314	-116.3566	33.4672	2.69	quartz monzonite
B315	-116.6509	33.6696	2.75	granodiorite
B317	-116.7907	33.6881	2.74	granodiorite
B318	-116.7537	33.6845	2.77	granodiorite
B319	-116.7565	33.6597	2.74	granodiorite
B320	-116.7189	33.6862	2.75	granodiorite
B321	-116.7142	33.6622	2.75	granodiorite
B322	-116.7142	33.6302	2.75	granodiorite
B323	-116.6837	33.6318	2.76	granodiorite
B324	-116.6472	33.6034	2.74	granodiorite
B325	-116.5308	33.4812	2.76	quartz diorite
B326	-116.4788	33.4226	2.80	quartz diorite
B327	-116.4309	33.4037	2.80	quartz diorite

Table 1. Samples, latitude and longitude, specific gravity and rock type of northern Peninsular Ranges granitic rocks

Sample	W. Longitude	N. Latitude	Specific gravity (g/cc)	Rock type
B328	-116.3801	33.3729	2.74	granodiorite
B329	-117.4952	33.9436	2.90	gabbro
B330	-117.5189	33.9155	2.66	quartz monzonite
B332	-117.4628	33.8546	2.66	quartz monzonite
B333	-117.4333	33.8266	2.67	quartz monzonite
B334	-117.3965	33.7961	2.66	quartz monzonite
B335	-117.3968	33.8551	2.90	gabbro
B336	-117.3597	33.9397	2.83	quartz diorite
B337	-117.3236	33.9697	2.73	granodiorite
B338	-117.2904	33.9986	2.71	quartz diorite
B339	-117.3261	33.9133	2.79	quartz diorite
B340	-117.2911	33.8856	2.79	quartz diorite
B341	-117.3287	33.8549	2.87	quartz diorite
B342	-117.3276	33.7971	2.83	quartz diorite
B343	-117.2913	33.8282	2.78	quartz diorite
B344	-117.2559	33.7985	2.79	quartz diorite
B345	-117.2909	33.7698	2.77	quartz diorite
B346	-117.3206	33.7411	2.68	granodiorite
B347	-117.2862	33.7123	2.83	quartz diorite
B348	-117.2847	33.6562	2.67	granodiorite
B349	-117.2506	33.6273	2.92	gabbro
B350	-117.2170	33.6540	2.72	granodiorite
B351	-117.1567	33.7134	2.72	granodiorite
B352	-117.1510	33.7718	2.80	quartz diorite
B353	-117.1180	33.7964	2.79	quartz diorite
B354	-117.1809	33.9183	2.75	granodiorite
B355	-117.1524	33.8906	2.73	granodiorite
B356	-117.1130	33.8521	2.71	granodiorite
B357	-117.0783	33.8247	2.82	quartz diorite
B358	-117.0438	33.7961	2.80	quartz diorite
B359	-117.0753	33.7674	2.81	quartz diorite
B360	-117.1167	33.7359	2.72	quartz diorite
B361	-117.1077	33.6804	2.73	quartz diorite
B362	-117.1813	33.6254	2.97	gabbro
B363	-117.2141	33.5987	2.81	granodiorite
B364	-117.1425	33.5963	2.68	granodiorite
B365	-117.1061	33.6249	2.91	gabbro
B366	-117.0760	33.6532	2.72	granodiorite
B367	-117.0717	33.5970	2.64	quartz monzonite
B369	-117.0021	33.5945	2.66	quartz monzonite
B370	-116.9734	33.6210	2.78	granodiorite
B371	-116.9365	33.6512	2.76	quartz diorite
B372	-116.9400	33.7075	2.75	quartz diorite
B373	-116.8971	33.6822	2.74	quartz diorite
B374	-116.8400	33.6258	2.80	quartz diorite
B375	-116.9077	33.6205	2.77	quartz diorite
B376	-116.9373	33.5965	2.80	quartz diorite
B377	-116.9786	33.5615	2.77	quartz diorite
B378	-117.0020	33.5371	2.75	quartz diorite
B379	-116.9754	33.5130	2.95	gabbro
B380	-116.9396	33.5398	2.76	quartz diorite

Table 1. Samples, latitude and longitude, specific gravity and rock type of northern Peninsular Ranges granitic rocks

Sample	W. Longitude	N. Latitude	Specific gravity (g/cc)	Rock type
B381	-116.9039	33.5669	2.78	quartz diorite
B382	-116.8757	33.5940	2.76	quartz diorite
B383	-116.8350	33.5696	2.77	quartz diorite
B384	-116.8719	33.5376	2.75	quartz diorite
B385	-116.9088	33.5092	2.77	quartz diorite
B386	-117.0048	33.4295	2.73	granodiorite
B387	-116.9758	33.3996	2.66	quartz monzonite
B388	-116.9383	33.3701	2.66	quartz monzonite
B389	-116.9083	33.3970	2.67	granodiorite
B390	-116.8346	33.4552	2.71	quartz diorite
B391	-116.8390	33.5126	2.69	granodiorite
B392	-116.7938	33.5463	2.74	granodiorite
B393	-116.7340	33.5972	2.98	gabbro
B394	-116.7017	33.5592	2.72	quartz diorite
B395	-116.7372	33.5397	2.74	quartz diorite
B396	-116.8032	33.4811	2.69	granodiorite
B397	-116.6371	33.5443	2.70	granodiorite
B398	-116.7021	33.5110	2.74	quartz diorite
B399	-116.7662	33.4549	2.73	granodiorite
B400	-116.8025	33.4260	2.72	quartz diorite
B401	-116.8045	33.3720	2.83	quartz diorite
B402	-116.8706	33.3697	2.74	granodiorite
B403	-116.9059	33.3399	2.86	quartz diorite
B404	-116.8704	33.3163	2.77	quartz diorite
B405	-116.7355	33.4450	2.77	quartz diorite
B406	-116.7020	33.4357	2.72	quartz monzonite
B407	-116.6010	33.4864	2.68	granodiorite
B408	-116.7010	33.4032	2.76	quartz diorite
B409	-116.7338	33.3716	2.75	granodiorite
B410	-116.7696	33.3407	2.74	quartz diorite
B411	-116.8035	33.3127	2.84	quartz diorite
B412	-116.8368	33.2818	2.83	quartz diorite
B413	-116.7634	33.2851	2.76	quartz diorite
B414	-116.7328	33.3111	3.04	gabbro
B415	-116.7000	33.3421	2.74	granodiorite
B416	-116.6659	33.3763	2.66	quartz monzonite
B417	-116.6335	33.3999	2.83	granodiorite
B418	-117.4681	34.0289	2.66	quartz monzonite
B419	-116.5415	33.4356	2.90	gabbro
B420	-116.5706	33.3992	2.82	quartz diorite
B421	-116.6006	33.3727	2.66	quartz monzonite
B422	-116.6345	33.3442	2.68	quartz monzonite
B423	-116.6632	33.3144	2.80	granodiorite
B424	-116.5647	33.3442	2.67	granodiorite
B425	-116.5306	33.3722	2.69	quartz monzonite
B426	-116.4962	33.3987	2.75	granodiorite
B427	-117.3980	34.0282	2.81	quartz diorite
B428	-117.4320	33.9975	2.63	quartz monzonite
B429	-117.5592	33.9437	2.77	quartz diorite
B430	-116.4623	33.3697	2.75	granodiorite
B431	-116.4212	33.3425	2.75	granodiorite

Table 1. Samples, latitude and longitude, specific gravity and rock type of northern Peninsular Ranges granitic rocks

Sample	W. Longitude	N. Latitude	Specific gravity (g/cc)	Rock type
B432	-116.4951	33.3409	2.79	quartz diorite
B433	-116.5324	33.3118	2.75	granodiorite
B434	-116.5997	33.3135	2.70	granodiorite
B435	-116.6359	33.2271	2.76	quartz diorire
B436	-116.6696	33.1995	2.72	quartz diorite
B437	-116.6339	33.1694	2.74	quartz diorite
B438	-116.6016	33.1965	2.76	quartz diorite
B439	-116.5679	33.2837	2.77	granodiorite
B440	-117.3612	33.8255	2.71	granodiorite
B441	-116.4256	33.2276	2.78	granodiorite
B442	-116.4269	33.1693	2.77	granodiorite
B447	-116.6155	33.4560	2.72	granodiorite
B448	-116.8684	33.4828	2.78	quartz diorite
B449	-116.8612	33.4236	2.75	quartz diorite
B450	-116.5316	33.2557	2.66	quartz monzonite
B451	-116.4293	33.2779	2.74	granodiorite
B452	-116.4699	33.2506	2.75	granodiorite
B453	-116.4957	33.2294	2.75	granodiorite
B454	-116.5313	33.1965	2.75	granodiorite
B455	-116.5011	33.1720	2.74	granodiorite
B456	-116.4611	33.1979	2.76	granodiorite
B458	-117.3559	33.6055	2.67	granodiorite
B460	-117.4703	33.7030	2.66	granodiorite
B461	-117.5092	33.6075	2.66	quartz monzonite
B462	-117.4612	33.6412	2.72	granodiorite
B463	-117.3911	33.6419	2.94	gabbro
B464	-117.4287	33.6117	2.69	quartz monzonite
B465	-117.3230	33.5820	2.66	quartz monzonite
B466	-117.3762	33.5546	2.68	granodiorite
B467	-117.3929	33.5244	2.88	gabbro
B468	-117.3220	33.5237	2.91	gabbro
B469	-117.3610	33.4944	2.66	granodiorite
B470	-117.3894	33.4576	2.66	granodiorite
B471	-117.3620	33.4339	2.64	quartz monzonite
B472	-117.3234	33.4624	2.67	granodiorite
B475	-117.3121	33.4281	2.67	granodiorite
B476	-117.3229	33.4068	2.69	granodiorite
B477	-117.3721	33.3756	2.95	gabbro
B478	-117.3490	33.3457	2.72	quartz diorite
B479	-117.2908	33.3748	2.67	granodiorite
B480	-117.2518	33.4042	2.67	granodiorite
B481	-117.2204	33.4337	2.96	gabbro
B482	-117.1504	33.4331	2.65	quartz monzonite
B483	-117.1823	33.4007	2.97	gabbro
B484	-117.2560	33.3448	2.82	quartz diorite
B485	-117.2920	33.3126	2.67	granodiorite
B486	-117.2579	33.2826	2.76	quartz diorite
B487	-117.1888	33.3457	2.83	quartz diorite
B488	-117.2567	33.3731	2.89	gabbro
B489	-117.1162	33.4014	2.65	quartz monzonite
B490	-117.0809	33.4321	2.65	quartz monzonite

Table 1. Samples, latitude and longitude, specific gravity and rock type of northern Peninsular Ranges granitic rocks

Sample	W. Longitude	N. Latitude	Specific gravity (g/cc)	Rock type
B491	-117.0812	33.3737	2.67	granodiorite
B492	-117.1178	33.3460	2.75	quartz diorite
B493	-117.1524	33.3145	2.68	granodiorite
B494	-117.1884	33.2849	2.77	quartz diorite
B495	-117.2561	33.2279	2.78	quartz diorite
B496	-117.1887	33.1711	2.80	quartz diorite
B497	-117.2135	33.1821	2.75	quartz diorite
B498	-117.1859	33.2279	2.85	quartz diorite
B499	-117.1520	33.2577	2.76	quartz diorite
B500	-117.0851	33.3309	2.79	quartz diorite
B501	-117.0457	33.3443	2.97	gabbro
B502	-117.0115	33.3167	2.72	quartz diorite
B503	-117.0461	33.2845	2.82	quartz diorite
B504	-117.0795	33.2537	2.67	quartz monzonite
B505	-117.1175	33.2275	2.88	gabbro
B506	-117.1529	33.1975	2.69	granodiorite
B508	-117.1148	33.1696	2.68	quartz diorite
B509	-117.0831	33.1981	2.94	gabbro
B510	-117.0462	33.2267	2.65	granodiorite
B511	-117.0101	33.2540	2.92	gabbro
B512	-116.9777	33.2827	2.92	gabbro
B513	-116.9360	33.2537	2.88	quartz diorite
B514	-116.9682	33.2295	2.85	quartz diorite
B515	-117.0103	33.1992	2.65	quartz monzonite
B516	-117.0455	33.1653	2.66	granodiorite
B517	-117.1135	33.1132	2.73	quartz diorite
B518	-117.1515	33.0862	2.70	quartz diorite
B519	-117.0845	33.0856	2.79	quartz diorite
B520	-117.0122	33.1392	2.69	quartz diorite
B522	-116.9395	33.1971	2.81	quartz diorite
B523	-116.9100	33.2198	2.82	quartz diorite
B524	-117.0760	33.0286	2.78	quartz diorite
B525	-117.0454	33.0494	2.77	quartz diorite
B528	-116.9719	33.1126	2.69	granodiorite
B529	-116.9403	33.1413	2.81	quartz diorite
B530	-116.9045	33.1714	2.82	quartz diorite
B531	-116.8738	33.1949	2.81	quartz diorite
B532	-116.8321	33.2296	2.94	gabbro
B533	-116.7688	33.2288	2.88	quartz diorite
B534	-116.8339	33.1718	2.93	gabbro
B535	-116.8728	33.1418	2.93	gabbro
B536	-116.9043	33.1131	2.89	quartz diorite
B537	-116.9379	33.0859	2.82	quartz diorite
B538	-116.9725	33.0555	2.68	granodiorite
B539	-117.0086	33.0242	2.69	granodiorite
B540	-116.9512	32.9641	2.67	granodiorite
B541	-116.9359	33.0283	2.69	granodiorite
B542	-116.9014	33.0546	2.71	granodiorite
B543	-116.8694	33.0866	2.90	quartz diorite
B544	-116.8349	33.1100	2.76	quartz diorite
B545	-116.8008	33.1424	2.92	gabbro

Table 1. Samples, latitude and longitude, specific gravity and rock type of northern Peninsular Ranges granitic rocks

Sample	W. Longitude	N. Latitude	Specific gravity (g/cc)	Rock type
B546	-116.7679	33.1698	2.76	granodiorite
B547	-116.7991	33.0836	2.80	quartz diorite
B548	-116.8325	33.0558	2.75	quartz diorite
B549	-116.9217	32.9703	2.71	granodiorite
B550	-116.9327	32.9562	2.64	quartz monzonite
B551	-116.9525	32.9217	2.70	granodiorite
B553	-116.8621	32.9557	2.64	quartz monzonite
B555	-116.7982	33.0255	2.75	quartz diorite
B556	-116.7655	33.0572	2.76	quartz diorite
B557	-116.7351	33.0836	2.79	quartz diorite

Samples from the U-Pb zircon age traverse of Premo and others (1997)

HSCZ	-117.5100	33.6038
SMZ	-117.3390	33.5122
SRPZ	-117.2644	33.5349
PV	-117.2871	33.6592
CZ-1		33.8088
GZ	-117.3439	33.7908
GZ-1	-117.3177	33.7765
GZ-2	-117.3003	33.7144
ADTZ	-117.3215	33.7367
DVZ	-117.2063	33.6712
MRZ	-117.3915	33.9848
MR	-117.3915	33.9848
VVZ	-117.2905	33.8860
BSZ	-117.2785	33.9891
LVZ	-117.0812	33.7847
GATZ	-117.0566	33.7243
SREZ	-116.9881	33.7126
RBZ	-116.9390	33.7180
WVRZ	-116.8846	33.5265
SJZ	-116.7220	33.7230
PFZ	-116.5203	33.5672
PFZ-1	-116.4271	33.5845
JMZ	-117.4700	34.0291

Notes: Na = Information is not available. Rock names are assigned using the modal mineral, granitic rock classification of Bateman and others (1963) by Baird and others (1979). The U-V coordinate system used by Baird and others (1979) to refer to sample localities was not used for this report. Latitude and longitude for each sample was digitally determined from stable base 1:250,000 scale, 1ºx2º topographic quadrangle maps furnished by A. K. Baird to D. M. Morton.

Table 2.Rubidium and strontium data for plutons of the northern Peninsular Ranges batholith, southern California

Sample	Rb(ppm)	Sr(ppm)	Rb/Sr	$^{87}Rb/^{86}Sr$	$^{87}Sr/^{86}Sr$	Age (Ma)	$(^{87}Sr/^{86}Sr)_o$	Pluton Name
B223	53.6	596	0.090	0.259	0.70605	94	0.7057	Unit 3
B224	104	382	0.273	0.790	0.70956	>94	0.7085	unassigned
B225	78.9	580	0.136	0.393	0.70655	94	0.7060	Unit 3
B226	95.8	520	0.184	0.532	0.71158	>94	0.7109	unassigned
B227	112	484	0.230	0.666	0.70847	94	0.7076	unassigned
B228	87.6	458	0.191	0.553	0.70770	94	0.7070	Unit 1
B229	50.2	614	0.082	0.237	0.70639	94	0.7061	unassigned
B230	102	477	0.215	0.622	0.70779	94	0.7070	Un it 1
B231	79.6	495	0.161	0.466	0.70724	94	0.7066	Unit 3
B232	110	575	0.191	0.553	0.70926	>94	0.7085	unassigned
B233	123	306	0.401	1.160	0.70857	94	0.7070	unassigned
B234	69.9	580	0.121	0.350	0.70759	94	0.7071	Unit 3
B236	132	270	0.488	1.412	0.70885	94	0.7070	Unit 3
B237	68.1	592	0.115	0.333	0.70755	94	0.7071	Unit 1
B238	89.2	480	0.186	0.538	0.70785	94	0.7071	Unit 1
B239	76.2	541	0.141	0.408	0.70781	94	0.7073	Unit 1
B240	73.6	539	0.136	0.393	0.70732	94	0.7068	Unit 3
B241	81.8	551	0.148	0.428	0.70731	94	0.7067	Unit 3
B242	80.7	553	0.146	0.422	0.70761	94	0.7071	Unit 3
B243	81	604	0.134	0.388	0.70747	94	0.7070	Unit 3
B244	59	523	0.113	0.327	0.70773	94	0.7073	Snow Creek
B245	92.7	396	0.234	0.677	0.70826	94	0.7074	Snow Creek
B246	82.6	493	0.167	0.483	0.70751	94	0.7072	Unit 3
B247	73.6	565	0.130	0.376	0.70710	94	0.7066	Unit 3
B248	75.7	570	0.133	0.385	0.70764	94	0.7071	Unit 3
B249	90	496	0.181	0.524	0.70758	94	0.7069	Unit 3
B250	94.8	497	0.191	0.553	0.70774	94	0.7070	Unit 1
B251	75.2	517	0.145	0.419	0.70762	94	0.7070	Unit 3
B252	75.2	537	0.140	0.405	0.70719	94	0.7067	Unit 3
B253	68.1	534	0.128	0.370	0.70810	94	0.7076	Unit 2
B254	65.5	569	0.115	0.333	0.70738	94	0.7069	Unit 3
B255	109	257	0.423	1.224	0.70822	94	0.7066	Unit 3
B256	88.1	476	0.185	0.535	0.70790	94	0.7072	Unit 1
B257	84.7	527	0.161	0.466	0.70768	94	0.7071	Unit 1
B258	88.1	519	0.170	0.492	0.70794	94	0.7073	Unit 1
B259	105	212	0.497	1.438	0.70864	94	0.7067	Unit 3
B260	90.3	348	0.260	0.752	0.70793	94	0.7069	Unit 3
B261	75.4	527	0.143	0.414	0.70786	94	0.7073	Unit 2
B262	94.5	266	0.355	1.027	0.70936	na	0.7074	shear zone sample
B263	80.7	195	0.415	1.201	0.70915	112R	0.7070	unassigned
B264	82.8	231	0.358	1.036	0.71014	94	0.7088	unassigned
B265	107	398	0.269	0.778	0.70819	112R	0.7070	unassigned
B266	134	153	0.874	2.529	0.71077	112R	0.7070	unassigned
B267	121	119	1.020	2.952	0.71194	112R	0.7070	unassigned
B268	114	245	0.468	1.354	0.70863	94	0.7069	unassigned
B269	53.6	614	0.087	0.252	0.70741	94	0.7071	Unit 2
B270	138	130	1.060	3.068	0.71054	100R	0.7061	Penrod Canyon
B271	130	118	1.100	3.183	0.71059	100R	0.7061	Penrod Canyon
B272	84.2	248	0.340	0.984	0.70729	100R	0.7061	Penrod Canyon
B273	47.9	547	0.088	0.255	0.70662	100R	0.7061	Penrod Canyon

Table 2.Rubidium and strontium data for plutons of the northern Peninsular Ranges batholith, southern California

Sample	Rb(ppm)	Sr(ppm)	Rb/Sr	$^{87}Rb/^{86}Sr$	$^{87}Sr/^{86}Sr$	Age (Ma)	$(^{87}Sr/^{86}Sr)_o$	Pluton Name
B274	94.8	488	0.194	0.561	0.70850	94?	0.7078	unassigned
B275	117	445	0.263	0.761	0.70864	na	0.7074	shear zone sample
B276	109	485	0.225	0.651	0.70862	na	0.7074	shear zone sample
B277	132	463	0.284	0.822	0.70897	98Z	0.7078	Pinyon Flat
B278	101	487	0.206	0.596	0.70893	98Z	0.7081	Pinyon Flat
B279	94.3	237	0.397	1.149	0.70795	35.7R	0.7074	possible Tertiary
B280	95.6	278	0.344	0.995	0.70786	35.7R	0.7074	possible Tertiary
B281	84.2	362	0.232	0.671	0.70770	35.7R	0.7074	possible Tertiary
B282	134	133	1.000	2.896	0.71634	na	0.7066	shear zone sample
B283	161	416	0.387	1.120	0.71039	na	0.7066	shear zone sample
B284	130	433	0.300	0.868	0.70915	94	0.7080	upper plate east
B285	105	492	0.213	0.616	0.70892	94	0.7081	upper plate east
B286	93.3	515	0.181	0.544	0.70847	94	0.7078	upper plate east
B287	97.7	461	0.212	0.614	0.70891	83	0.7081	upper plate east
B288	98.4	524	0.188	0.544	0.70855	83	0.7078	upper plate east
B289	104	530	0.196	0.567	0.70877	83	0.7080	upper plate east
B290	91.9	629	0.146	0.423	0.70846	83	0.7079	upper plate east
B291	106	522	0.202	0.585	0.70883	83	0.7081	upper plate east
B292	86.9	518	0.168	0.486	0.70877	83	0.7081	upper plate east
B293	106	538	0.197	0.570	0.70895	83	0.7082	upper plate east
B294	88.5	417	0.212	0.614	0.70903	83	0.7082	upper plate east
B295	103	481	0.214	0.619	0.70851	83	0.7077	upper plate east
B297	134	399	0.336	0.972	0.70885	83	0.7076	upper plate east
B298	104	454	0.230	0.666	0.70864	83	0.7078	upper plate east
B299	113	500	0.227	0.657	0.70884	83	0.7080	upper plate east
B300	72.3	591	0.122	0.353	0.70833	na	0.7083	Upper plate east
B301	105	431	0.243	0.703	0.70862	83	0.7077	upper plate east
B302	115	467	0.247	0.715	0.70922	84	0.7083	upper plate east
B303	102	546	0.186	0.538	0.70912	84	0.7084	upper plate west
B304	111	411	0.270	0.781	0.70878	84	0.7077	upper plate west
B305	153	367	0.416	1.204	0.70930	84	0.7077	upper plate west
B306	126	410	0.307	0.888	0.70892	84	0.7077	upper plate west
B307	87.6	447	0.196	0.567	0.70843	84	0.7077	upper plate west
B308	107	469	0.227	0.657	0.70920	84	0.7083	upper plate west
B309	112	430	0.260	0.752	0.70878	84	0.7078	upper plate west
B310	121	430	0.281	0.813	0.70869	84	0.7076	upper plate west
B311	94.4	503	0.188	0.544	0.70886	84	0.7080	upper plate west
B312	109	31.9	3.400	9.850	0.72098	98.5R	0.7073	Buck Ridge
B313	134	97.8	1.370	3.966	0.71305	98.5R	0.7073	Buck Ridge
B314	145	143	1.020	2.952	0.71139	98.5R	0.7073	Buck Ridge
B315	65.7	486	0.135	0.391	0.70717	94	0.7067	Unit 2
B317	49.6	548	0.091	0.262	0.70714	94	0.7068	Unit 1
B318	58	568	0.102	0.295	0.70760	94	0.7074	Unit 1
B319	51.1	540	0.095	0.274	0.70730	94	0.7069	Unit 1
B320	56.2	588	0.096	0.276	0.70764	94	0.7073	Unit 2
B321	53.3	574	0.093	0.268	0.70752	94	0.7072	Unit 1
B322	53.5	579	0.093	0.268	0.70798	94	0.7076	Unit 1
B323	49.1	630	0.076	0.221	0.70678	94	0.7065	Unit 1
B324	44.7	504	0.089	0.257	0.70635	94	0.7060	Unit 1

End San Jacinto block start Perris block

Table 2.Rubidium and strontium data for plutons of the northern Peninsular Ranges batholith, southern California

Sample	Rb(ppm)	Sr(ppm)	Rb/Sr	$^{87}Rb/^{86}Sr$	$^{87}Sr/^{86}Sr$	Age (Ma)	$(^{87}Sr/^{86}Sr)_o$	Pluton Name
B325	98.9	332	0.289	0.836	0.70781	100	0.7066	unassigned
B326	104	265	0.393	1.137	0.70680	100	0.7051	unassigned
B326	109	265	0.393	1.137	0.70680	100	0.7051	unassigned
B327	83.9	305	0.276	0.798	0.70617	100	0.7051	unassigned
B328	94.9	259	0.366	1.059	0.70652	100	0.7051	unassigned
B329	10.2	320	0.032	0.092	0.70445	109	0.7043	Cajalco (gabbro)
B330	164	92.2	1.780	5.151	0.71249	109R(108Z)	0.7044	Cajalco
B332	154	122	1.260	3.646	0.71009	109R(108Z)	0.7044	Cajalco
B333	105	140	0.748	2.165	0.70771	109R(108Z)	0.7044	Cajalco
B334	185	99.3	1.860	5.385	0.71264	109R(108Z)	0.7044	Cajalco
B335	6.5	377	0.017	0.049	0.70458	109R(108Z)	0.7045	Cajalco
B336	53.8	278	0.193	0.558	0.70534	129R(106Z)	0.7045	Val Verde
B337	85.6	217	0.395	1.143	0.70650	129R(106Z)	0.7048	Val Verde
B338	95.5	285	0.335	0.969	0.70639	98.6R(98Z)	0.7051	Box Springs
B339	38.1	363	0.105	0.304	0.70496	129R(106Z)	0.7045	Val Verde
B340	55.2	312	0.177	0.512	0.70535	129R106Z)	0.7046	Val Verde
B341	43	313	0.137	0.396	0.70508	129R(106Z)	0.7045	Val Verde
B342	65	276	0.235	0.680	0.70516	110Z	0.7045	Gavilan
B343	64.5	286	0.225	0.651	0.70556	129R(106Z)	0.7046	Val Verde
B344	66.7	296	0.226	0.653	0.70552	129R(106Z)	0.7045	Val Verde
B345	46.7	217	0.215	0.620	0.70608	108Z	0.7052	Gavilan
B346	124	117	1.060	3.070	0.70954	110Z	0.7044	Arroyo del Torro
B347	41.5	252	0.165	0.477	0.70527	108Z	0.7045	Gavilan
B348	77.9	122	0.638	1.846	0.70751	110Z	0.7046	Paloma Valley
B349	14.6	299	0.049	0.141	0.70381	110Z	0.7036	Gabbro, Paloma Valley.
B350	70.5	207	0.340	0.984	0.70617	118Z	0.7045	Domenigoni Valley
B351	75.1	258	0.291	0.841	0.7051	118Z	0.7039	Domenigoni Valley
B352	73.8	277	0.267	0.772	0.70600	95R(99Z)	0.7049	Lakeview
B353	41	342	0.120	0.347	0.70545	95R(99Z)	0.7050	Lakeview
B354	76.9	243	0.316	0.914	0.70653	100	0.7052	unassigned
B355	99	212	0.468	1.354	0.70675	100	0.7048	unassigned
B356	94.9	197	0.481	1.392	0.70752	100	0.7055	unassigned
B357	49.1	294	0.167	0.483	0.70541	95R(99Z)	0.7047	Lakeview
B358	53	278	0.190	0.549	0.70557	95R(99Z)	0.7048	Lakeview
B359	56.5	293	0.193	0.558	0.70564	95R(99Z)	0.7049	Lakeview
B360	48.1	229	0.210	0.608	0.70501	118Z	0.7040	Domenigoni Valley
B361	56	219	0.255	0.738	0.70517	118Z	0.7041	Domenigoni Valley
B362	5	306	0.016	0.047	0.70378	110Z	0.7037	Gabbro, Paloma Valley
B363	15.6	360	0.043	0.125	0.70377	110Z	0.7036	Paloma Valley
B364	76.9	143	0.539	1.559	0.70602	110Z	0.7036	Paloma Valley
B365	8.7	322	0.027	0.078	0.70371	110Z	0.7036	Gabbro, Paloma Valley
B366	43.2	233	0.186	0.538	0.70448	118Z	0.7037	Dominogoni Valley
B367	132	56.2	2.350	6.806	0.71719	110Z	0.7066	Paloma Valley
B369	104	90.4	1.150	3.328	0.70966	107.5R	0.7046	unassigned
B370	98	288	0.340	0.984	0.70671	116R(97Z)	0.7052	Wilson Valley
B371	33.9	555	0.061	0.177	0.70547	116R(97Z)	0.7052	Wilson Valley
B372	68.8	529	0.130	0.376	0.70752	99Z	0.7070	Ramona Bowl
B373	38.1	548	0.070	0.201	0.70552	116R(97Z)	0.7052	Wilson Valley
B374	28.1	430	0.065	0.189	0.70511	100	0.7048	unassigned
B375	40.8	547	0.075	0.216	0.70554	116R(97Z)	0.7052	Wilson Valley

Table 2.Rubidium and strontium data for plutons of the northern Peninsular Ranges batholith, southern California

Sample	Rb(ppm)	Sr(ppm)	Rb/Sr	$^{87}Rb/^{86}Sr$	$^{87}Sr/^{86}Sr$	Age (Ma)	$(^{87}Sr/^{86}Sr)_o$	Pluton Name
B376	83.4	285	0.292	0.845	0.70656	116R(97Z)	0.7052	Wilson Valley
B377	20	470	0.043	0.123	0.70464	116R(97Z)	0.7046	unassigned
B378	33	434	0.076	0.220	0.70483	107.5R	0.7046	unassigned
B379	0.8	361	0.002	0.006	0.70336	100	0.7034	gabbro
B380	34.9	451	0.077	0.224	0.70468	107.5R	0.7046	unassigned
B381	32.7	567	0.058	0.167	0.70532	116R(97Z)	0.7051	Wilson Valley
B382	42.8	544	0.077	0.222	0.70553	116R(97Z)	0.7052	Wilson Valley
B383	41.3	561	0.074	0.213	0.70532	100	0.7050	unassigned
B384	45	534	0.084	0.244	0.70543	116R(97Z)	0.7051	Wilson Valley
B385	39.1	528	0.074	0.214	0.70544	116R(97Z)	0.7051	Wilson Valley
B386	12.6	330	0.038	0.111	0.70344	130R	0.7032	unassigned
B387	105	106	0.990	2.865	0.70868	130R	0.7032	unassigned
B388	107	94.5	1.130	3.270	0.70948	130R	0.7032	unassigned
B389	107	118	0.901	2.607	0.70789	130R	0.7032	unassigned
B390	42.3	544	0.078	0.225	0.70514	107R	0.7049	unassigned
B391	45.7	429	0.107	0.310	0.70539	100	0.7050	unassigned
B392	77.7	461	0.169	0.489	0.70610	100	0.7054	unassigned
B393	5.5	296	0.019	0.054	0.70317	100	0.7031	Gabbro
B394	68.5	475	0.144	0.417	0.70624	135R	0.7055	unassigned
B395	53.3	545	0.098	0.283	0.70597	135R	0.7055	unassigned
B396	75.4	412	0.183	0.529	0.70641	135R	0.7055	unassigned
B397	92.8	418	0.222	0.642	0.70638	100	0.7055	unassigned
B398	64.7	523	0.124	0.359	0.70607	135R	0.7055	unassigned
B399	81.6	422	0.193	0.558	0.70650	135R	0.7055	unassigned
B400	44.2	535	0.083	0.239	0.70538	107R	0.7049	unassigned
B401	57.7	308	0.187	0.541	0.70507	100	0.7043	unassigned
B402	123	154	0.798	2.310	0.71523	100	0.7120	unassigned
B403	47	325	0.145	0.419	0.70416	130R	0.7032	unassigned
B404	72.8	313	0.233	0.674	0.70537	100	0.7044	unassigned
B405	89.4	364	0.245	0.709	0.70603	107R	0.7049	unassigned
B406	133	213	0.625	1.810	0.71582	100	0.7133	unassigned
B407	102	351	0.291	0.842	0.70784	100	0.7066	unassigned
B408	85.5	458	0.187	0.541	0.70562	107R	0.7049	unassigned
B409	69.8	431	0.162	0.469	0.70555	107R	0.7049	unassigned
B410	66	331	0.199	0.575	0.70545	100	0.7046	unassigned
B411	22.7	402	0.057	0.163	0.70445	100	0.7042	unassigned
B412	29.2	374	0.078	0.226	0.70448	100	0.7042	unassigned
B413	87.8	283	0.310	0.897	0.70592	100	0.7046	unassigned
B414	6	455	0.013	0.038	0.70405	100	0.7040	gabbro
B415	104	224	0.464	1.342	0.70685	100	0.7049	unassigned
B416	123	239	0.513	1.484	0.70737	100	0.7053	unassigned
B417	77.4	282	0.274	0.792	0.70646	92.5R	0.7054	unassigned
B418	197	117	1.680	4.863	0.71260	103Z	0.7055	Jurupa Mountai
B419	19.8	244	0.081	0.235	0.70474	100	0.7044	unassigned
B420	57.7	350	0.165	0.477	0.70616	92.5R	0.7054	unassigned
B421	148	81.8	1.810	5.242	0.71597	100	0.7085	unassigned
B422	162	151	1.070	3.097	0.70925	100	0.7048	unassigned
B423	98.2	252	0.390	1.128	0.70593	100	0.7043	unassigned
B424	93.3	280	0.333	0.963	0.70634	100	0.7050	unassigned
B425	8.9	326	0.027	0.079	0.70456	100	0.7045	unassigned

Table 2.Rubidium and strontium data for plutons of the northern Peninsular Ranges batholith, southern California

Sample	Rb(ppm)	Sr(ppm)	Rb/Sr	$^{87}Rb/^{86}Sr$	$^{87}Sr/^{86}Sr$	Age (Ma)	$(^{87}Sr/^{86}Sr)_o$	Pluton Name
B426	86.8	323	0.269	0.778	0.70612	100	0.7050	unassigned
B427	33.7	298	0.113	0.327	0.70496	98.7	0.7045	unassigned
B428	215	19.1	11.256	32.838	0.75059	109Z	0.7045	Rubidoux Muntain
B429	1	293	0.003	0.009	0.70477	100	0.7048	unassigned
B430	91.3	306	0.298	0.862	0.70637	100	0.7052	unassigned
B431	94.4	286	0.330	0.955	0.70608	100	0.7047	unassigned
B432	68.2	398	0.171	0.495	0.70611	100	0.7054	unassigned
B433	75.9	354	0.214	0.619	0.70573	100	0.7049	unassigned
B434	79.2	276	0.286	0.827	0.70651	100	0.7053	unassigned
B435	50.8	549	0.093	0.268	0.70514	100	0.7047	unassigned
B436	61.5	553	0.111	0.321	0.70511	100	0.7047	unassigned
B437	46.9	499	0.094	0.272	0.70506	100	0.7047	unassigned
B438	69.3	499	0.139	0.402	0.70525	100	0.7047	unassigned
B439	66.7	498	0.134	0.388	0.70632	100	0.7058	unassigned
B440	69	197	0.350	1.013	0.70606	100	0.7054	unassigned
B441	63.9	600	0.106	0.307	0.70665	104.5R	0.7062	Pinyon Ridge
B442	74.6	552	0.135	0.391	0.70675	104.5R	0.7062	Pinyon Ridge
B447	88.1	408	0.216	0.625	0.70656	100	0.7057	unassigned
B448	29.7	574	0.052	0.149	0.70513	100	0.7049	unassigned
B449	76.9	354	0.217	0.628	0.70688	100	0.7060	unassigned
B450	190	148	1.280	3.704	0.71166	104.5R	0.7062	Pinyon Ridge
B451	84.2	347	0.243	0.703	0.70773	104R	0.7067	unassigned
B452	84.4	485	0.174	0.503	0.70692	104.5R	0.7062	Pinyon Ridge
B453	102	443	0.231	0.668	0.70720	104.5R	0.7062	Pinyon Ridge
B454	82.3	506	0.163	0.471	0.70787	104R	0.7072	unassigned
B455	101	353	0.287	0.830	0.70780	104R	0.7066	unassigned
B456	65.1	588	0.111	0.321	0.70665	104.5R	0.7062	Pinyon Ridge
End Perris block begin Santa Ana block								
B458	70.3	117	0.602	1.740	0.70654	122Z	0.7043	Santa Rosa
B460	67.2	120	0.561	1.620	0.70751	124R	0.7047	Woodson Mountain
B461	126	135	0.930	2.691	0.70808	119Z	0.7035	Hot Springs Canyon
B462	99.5	155	0.640	1.851	0.70761	122Z	0.7044	Santa Rosa
B463	6.2	344	0.018	0.052	0.70396	122Z	0.7038	gabbro
B464	112	143	0.782	2.263	0.70825	122Z	0.7043	Santa Rosa
B465	107	107	1.000	2.893	0.70863	122Z	0.7036	Santa Rosa
B466	63	115	0.548	1.585	0.70674	122Z	0.7040	Santa Rosa
B467	6.4	370	0.017	0.050	0.70357	100	0.7036	gabbro
B468	7.6	230	0.033	0.095	0.70401	100	0.7038	gabbro
B469	101	114	0.888	2.570	0.70809	106.3R	0.7041	Roblar
B470	111	117	0.951	2.752	0.70822	106.3R	0.7041	Roblar
B471	140	49.3	2.840	8.222	0.71656	106.3R	0.7041	Roblar
B472	89.2	164	0.543	1.571	0.70612	124R	0.7036	Woodson Mountain
B475	114	101	1.130	3.270	0.70907	124R	0.7036	Woodson Mountain
B476	107	134	0.797	2.306	0.70782	124R	0.7036	Woodson Mountain
B477	1	419	0.002	0.006	0.70353	124R	0.7035	gabbro
B478	78.4	229	0.342	0.989	0.70518	105.2R	0.7038	Bonsall
B479	110	115	0.952	2.755	0.70871	124R	0.7036	Woodson Mountain
B480	79.5	146	0.544	1.573	0.70648	124R	0.7036	Woodson Mountain
B481	4.5	340	0.013	0.038	0.70381	124R	0.7036	gabbro
B482	100	56.2	1.780	5.151	0.71242	124R	0.7036	Woodson Mountain

Table 2.Rubidium and strontium data for plutons of the northern Peninsular Ranges batholith, southern California

Sample	Rb(ppm)	Sr(ppm)	Rb/Sr	$^{87}Rb/^{86}Sr$	$^{87}Sr/^{86}Sr$	Age (Ma)	$(^{87}Sr/^{86}Sr)_o$	Pluton Name
B483	2.6	415	0.006	0.018	0.70376	124R	0.7036	gabbro
B483	2.3	415	0.006	0.016	0.70374	124R	0.7036	gabbro
B484	28	342	0.082	0.237	0.70403	105.2R	0.7038	Bonsall
B485	142	144	0.987	2.856	0.70800	105.2R	0.7038	Bonsall
B486	50.6	288	0.176	0.509	0.70440	124R	0.7036	Woodson Mountain
B487	23	307	0.075	0.217	0.70419	105.2R	0.7038	Bonsall
B488	0.8	388	0.002	0.006	0.70368	105.2R	0.7038	gabbro
B489	98.2	89.5	1.100	3.183	0.70945	124R	0.7036	Woodson Mountain
B490	118	102	1.160	3.357	0.70944	124R	0.7036	Woodson Mountain
B491	77.3	130	0.592	1.713	0.70642	124R	0.7036	Woodson Mountain
B492	79.7	253	0.315	0.911	0.70520	105.2R	0.7038	Bonsall
B493	53.8	182	0.295	0.853	0.70503	124R	0.7036	Indian Mountain
B494	76.9	263	0.293	0.847	0.70497	105.2R	0.7038	Bonsall
B495	58.7	277	0.212	0.613	0.70462	105.2R	0.7038	Bonsall
B496	36.6	188	0.195	0.564	0.70454	117R	0.7036	Green Valley
B497	65.5	260	0.252	0.729	0.70492	117R	0.7036	Green Valley
B498	62	248	0.250	0.723	0.70482	117R	0.7036	quartz diorite
B499	42	237	0.177	0.512	0.70460	124R	0.7036	Woodson Mountain
B500	80	275	0.291	0.842	0.70480	124R	0.7036	Indian Mountain
B501	2	450	0.005	0.013	0.70371	117R	0.7037	Gabbro
B502	12.6	387	0.033	0.094	0.70389	117R	0.7037	quartz diorite
B503	41.3	262	0.157	0.454	0.70442	105.2R	0.7038	Bonsall
B504	93.1	132	0.707	2.045	0.70701	124R	0.7036	Woodson Mountain
B505	9.7	323	0.030	0.087	0.70371	117R	0.7037	San Marcos
B506	64.7	171	0.379	1.096	0.70550	124R	0.7036	Woodson Mountain
B508	72.8	157	0.463	1.339	0.70581	117R	0.7036	Green Valley
B509	12.6	352	0.036	0.104	0.70376	117R	0.7037	gabbro
B510	73.3	156	0.471	1.363	0.70588	124R	0.7036	Woodson Mountain
B511	11.4	340	0.034	0.097	0.70382	117R	0.7037	gabbro
B512	6	363	0.016	0.046	0.70377	117R	0.7037	gabbro
B513	16.6	319	0.052	0.150	0.70390	105.2R	0.7038	Bonsall?
B514	37.1	291	0.128	0.370	0.70429	105.2R	0.7038	Bonsall?
B515	71.8	72.7	0.987	2.850	0.70894	113.4R	0.7036	Lake Wolford
B516	57	113	0.504	1.458	0.70623	113.4R	0.7036	Lake Wolford
B517	70.6	178	0.396	1.146	0.70555	117R	0.7036	Green Valley
B517	72.6	178	0.407	1.177	0.70555	117R	0.7036	Green Valley
B518	46.7	293	0.159	0.460	0.70424	100	0.7036	Escondido Creek
B519	61.7	256	0.241	0.697	0.70476	117R	0.7036	Green Valley
B520	73.8	143	0.518	1.499	0.70606	113.4R	0.7036	Lake Wolford
B522	40.1	289	0.139	0.402	0.70438	105.2R	0.7038	Bonsall
B523	30.2	290	0.104	0.308	0.70415	105.2R	0.7038	Bonsall
B524	42.3	254	0.166	0.480	0.70439	117R	0.7036	Green Valley
B525	64.5	202	0.319	0.922	0.70517	117R	0.7036	Green Valley
B528	41.8	151	0.277	0.801	0.70497	124R	0.7036	Woodson Mountain
B529	69.8	212	0.329	0.952	0.70547	117R	0.7036	Green Valley
B530	47.4	268	0.177	0.512	0.70463	113.4R	0.7036	Lake Wolford
B531	76.1	220	0.346	1.001	0.70545	105.2R	0.7038	Bonsall
B532	24	284	0.085	0.245	0.70421	105.2R	0.7038	Bonsall
B533	20.3	368	0.055	0.159	0.70486	105R	0.7046	contam. bonsall
B534	22.7	303	0.075	0.217	0.70426	105.2R	0.7038	Bonsall

Table 2.Rubidium and strontium data for plutons of the northern Peninsular Ranges batholith, southern California

B535	4	249	0.016	0.046	0.70413	100	0.7041	gabbro
Sample	Rb(ppm)	Sr(ppm)	Rb/Sr	$^{87}Rb/^{86}Sr$	$^{87}Sr/^{86}Sr$	Age (Ma)	$(^{87}Sr/^{86}Sr)_o$	Pluton Name
B536	24.7	302	0.082	0.236	0.70424	117R	0.7036	Green Valley
B537	56	234	0.240	0.694	0.70503	117R	0.7036	Green Valley
B538	80	149	0.536	1.550	0.70630	124R	0.7036	Woodson Mountain
B539	53	197	0.269	0.778	0.70497	124R	0.7036	Woodson Mountain
B540	86.5	150	0.578	1.672	0.70644	124R	0.7036	Woodson Mountain
B541	97.7	142	0.687	1.987	0.70693	124R	0.7036	Woodson Mountain
B542	16.1	220	0.073	0.212	0.70388	124R	0.7036	Woodson Mountain
B543	34.7	262	0.132	0.382	0.70474	105R	0.7043	contaminated Bonsall
B544	26.7	288	0.093	0.269	0.70417	105.2R	0.7038	Bonsall
B545	24.5	315	0.078	0.225	0.70450	92.5R	0.7043	Ramona outlier
B546	74.6	298	0.251	0.726	0.70516	92.5R	0.7043	Ramona outlier
B547	48.1	401	0.120	0.347	0.70500	94Z	0.7045	Ramona
B548	45.2	457	0.099	0.286	0.70437	94Z	0.7040	Ramona
B549	95.4	163	0.587	1.698	0.70635	113.4R	0.7036	Lake Wolford
B550	140	14.9	9.400	27.307	0.74771	113.4R	0.7036	Lake Wolford
B551	50.6	145	0.349	1.010	0.70533	113.4R	0.7036	Lake Wolford
B553	143	35.4	4.050	11.729	0.72211	113.4R	0.7036	Lake Wolford
B555	45.2	475	0.095	0.275	0.70431	113.4R	0.7036	Lake Wolford
B556	59.5	340	0.175	0.506	0.70495	94Z	0.7042	Ramona
B557	52.8	457	0.115	0.333	0.70472	94Z	0.7043	Ramona
End Baird specimens, begin zircon traverse								
HSCZ(SA)	105	114	0.920	2.662	0.70988	119Z	0.7054	Hot Springs Creek
SMZ(SA)	75.6	142	0.532	1.539	0.70690	120Z	0.7043	Squaw Mountain
SRPZ(SA)	85.9	216	0.398	1.151	0.70614	122Z	0.7041	Santa Rosa
PVZ(P)	69.5	205	0.339	0.981	0.70731	110Z	0.7058	Paloma Valley
CZ-1(P)	137	145	0.950	2.749	0.70890	108Z	0.7047	Cajalco
GZ (P)	65.8	276	0.238	0.689	0.70543	108Z	0.7044	Gavilan
GZ-1 (P)	74.8	285	0.262	0.758	0.70523	109Z	0.7041	Gavilan
GZ-2 (P)	135	122	1.110	3.212	0.71135	113Z	0.7062	Gavilan
ADTZ (P)	103	128	0.804	2.327	0.70948	110Z	0.7059	Arroyo Del Torro
DVZ (P)	53.3	241	0.221	0.639	0.70530	118Z	0.7042	Domenigoni
JMZ (P)	76.2	225	0.338	0.978	0.70617	103Z	0.7047	Jurupa Mountain
MRZ (P)	148	92.5	1.600	4.632	0.71211	109Z	0.7049	Rubidoux
EL-38-167(P)	159	105	1.509	4.370	0.71210	109Z	0.7053	Rubidoux
VVZ (P)	56.5	315	0.179	0.518	0.70554	106Z	0.7048	Val Verde
BSZ (P)	40.7	428	0.095	0.275	0.70555	98Z	0.7052	Box Springs
LVZ (P)	23.8	358	0.066	0.192	0.70523	99Z	0.7050	Lakeview Mountain
GATZ (P)	2.3	308	0.008	0.022	0.70461	99Z	0.7046	Green Acres
SREZ (P)	18.8	604	0.031	0.090	0.70529	99Z	0.7052	Searles Ridge
RBZ (P)	46.4	570	0.081	0.235	0.70666	99Z	0.7063	Ramona Bowl
WVRS (P)	31.6	595	0.053	0.154	0.70543	97Z	0.7052	Wilson Valley
SJZ (SJ)	77.5	424	0.183	0.530	0.70816	94Z	0.7075	San Jacinto
PFZ (SJ)	41.3	615	0.067	0.194	0.70730	98Z	0.7070	Pinyon Flat
PFZ-1 (SJ)	91.6	465	0.197	0.570	0.70849	84Z	0.7078	Pinyon Flat
PHZ (SJ)	108	405	0.266	0.769	0.70887	83Z	0.7080	Point Happy

Notes: Rock types are identified in Table 1. Pluton names: San Jacinto block; Below the shear zone, Units 1-3 for the San Jacinto pluton and other pluton names are from Hill and Silver (1988). Above the shear zone the plutons are informally separated into an east and west group. The Point Happy and Pinyon Flat pluton names are from Premo and others (1997). Perris block: Pluton names are from Premo and others (1997) and references therein. Santa Ana block: Pluton names are from Larsen (1948) and Premo and others (1997). U-Pb zircon and Rb-Sr whole-rock age assignments are identified by either Z or by R after the age. An age of 100 m.y. was assumed for all specimens without physical age data. Specimen EL-38-167 (P) is from Rubidoux Mountain pluton collected by E.S. Larsen Jr., data from Kistler and others (1973).

Table 3. U, Th, Pb concentrations, initial Pb and Sr isotopic compositions, and $\delta^{18}O$ permil values for whole-rock specimens of plutons of the northern Peninsular Ranges batholith

				WR Present-Day Pb ratios					WR Age-Corrected Pb ratios					
Sample	Pb (ppm)	U (ppm)	Th (ppm)	$^{206}Pb/^{204}Pb$	$^{207}Pb/^{204}Pb$	$^{208}Pb/^{204}Pb$	$^{238}U/^{204}Pb$	$^{232}Th/^{204}Pb$	$^{206}Pb/^{204}Pb$	$^{207}Pb/^{204}Pb$	$^{208}Pb/^{204}Pb$	Age(Ma)	δ^{18} O	Sri
B223	14.40	1.54	3.93	19.263	15.676	38.870	7.000	18.2	19.161	15.671	38.785	94.0	10.1	0.7057
B229	11.56	1.59	4.41	19.276	15.698	38.933	8.971	25.5	19.144	15.691	38.814	94.0		0.7061
B231	11.10	1.78	9.54	19.349	15.686	38.998	10.500	57.6	19.195	15.678	38.729	94.0	10.4	0.7066
B232	11.20	2.31	16.60	19.598	15.717	39.244	13.600	100.0	19.399	15.707	38.778	94.0	10.6	0.7085
B240	13.20	2.14	6.71	19.399	15.691	39.064	10.600	34.1	19.243	15.683	38.905	94.0	10.3	0.7068
B245	7.48	1.27	7.64	19.408	15.698	38.989	11.101	68.5	19.244	15.690	38.669	94.0		0.7074
B253	11.60	1.57	6.08	19.427	15.696	39.070	8.900	35.2	19.296	15.689	38.906	94.0	10.0	0.7076
B255	16.94	0.95	8.83	19.237	15.675	38.986	3.657	34.9	19.183	15.672	38.823	94.0	9.5	0.7066
B257	13.20	1.65	5.89	19.421	15.689	38.985	8.200	29.9	19.300	15.683	38.845	94.0	10.0	0.7071
B258												94.0	9.8	0.7073
B259												94.0	9.8	0.7067
B260												94.0	9.4	0.7069
B264	18.50	2.05	8.66	19.580	15.708	39.089	7.300	31.5	19.473	15.703	38.942	94.0	10.8	0.7088
B265	9.30	1.84	10.26	19.388	15.693	39.036	12.940	74.0	19.197	15.684	38.691	112.0	9.2	0.7069
B266	25.20	3.87	9.14	19.336	15.678	38.955	10.000	24.3	19.189	15.671	38.841	112.0	10.6	0.7069
B267												112.0	11.2	0.7069
B268												94.0	9.0	0.7069
B270	17.10	2.22	12.69	19.244	15.655	38.780	8.441	49.5	19.120	15.650	38.549	100.0	10.5	0.7061
B271												100.0	11.1	0.7061
B276												na	9.6	0.7074
B277	14.47	1.69	10.21	19.581	15.713	39.175	7.674	47.6	19.473	15.708	38.962	98.0	9.3	0.7078
B280	12.40	2.38	12.27	19.348	15.689	39.195	12.600	66.5	19.172	15.680	38.898	35.7	9.7	0.7074
B288	9.20	1.61	17.85	19.440	15.699	39.443	11.500	131.0	19.278	15.691	38.858	83.0	8.6	0.7078
B290	12.67	3.30	11.89	19.464	15.698	39.152	17.079	63.1	19.223	15.686	38.870	83.0		0.7079
B292	9.00	2.41	9.88	19.373	15.688	39.110	17.500	73.7	19.126	15.676	38.781	83.0	8.9	0.7081
B297	15.00	2.98	22.35	19.636	15.715	39.395	13.100	100.9	19.452	15.706	38.944	83.0	9.1	0.7076
B298	11.20	2.13	15.02	19.591	15.705	39.255	12.600	90.9	19.414	15.696	38.849	83.0	8.9	0.7078
B300	9.80	1.67	1.75	19.500	15.725	39.074	11.200	12.0	19.343	15.717	39.021	na	8.9	0.7083
B301												83.0	8.7	0.7077
B302	12.44	5.16	36.37	19.613	15.714	39.488	27.381	198.0	19.228	15.695	38.604	84.0	8.8	0.7083
B306	17.40	2.97	31.70	19.634	15.710	39.304	11.200	123.1	19.476	15.702	38.755	84.0	8.6	0.7077
B307												84.0	8.6	0.7077
B310	13.01	3.83	23.08	19.684	15.715	39.539	19.464	120.3	19.410	15.702	39.002	84.0	8.3	0.7076

Table 3. U, Th, Pb concentrations, initial Pb and Sr isotopic compositions, and $\delta^{18}O$ permil values for whole-rock specimens of plutons of the northern Peninsular Ranges batholith

				WR Present-Day Pb ratios					WR Age-Corrected Pb ratios					
Sample	Pb (ppm)	U (ppm)	Th (ppm)	$^{206}Pb/^{204}Pb$	$^{207}Pb/^{204}Pb$	$^{208}Pb/^{204}Pb$	$^{238}U/^{204}Pb$	$^{232}Th/^{204}Pb$	$^{206}Pb/^{204}Pb$	$^{207}Pb/^{204}Pb$	$^{208}Pb/^{204}Pb$	Age(Ma)	$\delta^{18}O$	
B312	21.30	0.82	7.61	19.052	15.630	38.658	2.500	23.8	19.014	15.629	38.544	98.5	10.1	0.7073
B313	15.70	0.39	5.56	19.142	15.648	38.760	1.600	23.6	19.118	15.647	38.647	98.5	12.8	0.7073
B314	29.90	1.01	20.56	19.369	15.702	38.951	2.100	46.0	19.335	15.700	38.730	98.5	11.0	0.7073
B318	10.20	2.58	7.03	19.368	15.686	38.974	16.500	46.2	19.125	15.674	38.758	94.0	9.9	0.7074
B324	8.40	1.35	7.40	19.223	15.655	39.065	10.500	59.0	19.069	15.648	38.790	94.0	9.7	0.7060
					Perris block									
B330	10.48	4.39	15.12	19.406	15.646	39.083	27.403	96.8	18.977	15.626	38.603	108Z		0.7044
B334	14.60	2.92	18.41	19.301	15.629	38.918	13.000	84.1	19.092	15.619	38.489	108Z		0.7044
B336	7.46	1.12	2.97	18.818	15.614	38.573	9.674	26.3	18.667	15.607	38.442	106Z		0.7045
B340	7.20	0.77	6.20	18.919	15.631	38.913	7.000	57.4	18.790	15.625	38.577	106Z		0.7046
B341	6.10	1.14	4.03	18.971	15.662	38.662	12.100	44.1	18.746	15.651	38.404	106Z		0.7045
B342	7.90	1.87	6.02	19.014	15.630	38.779	15.400	50.8	18.773	15.619	38.527	110.0		0.7045
B343	8.20	0.76	7.34	18.981	15.626	38.806	6.000	59.8	18.869	15.621	38.456	106Z		0.7046
B345	9.60	1.21	3.62	18.973	15.627	38.719	8.200	25.1	18.845	15.621	38.594	108Z		0.7052
B351	6.60	0.99	5.07	19.058	15.610	38.722	9.700	50.8	18.907	15.603	38.470	118Z		0.7039
B354	12.60	1.92	4.68	18.968	15.637	38.751	9.800	24.6	18.814	15.630	38.629	35.0		0.7061
B356	65.20	2.40	4.72	18.863	15.639	38.665	2.400	4.8	18.826	15.638	38.642	100.0		0.7055
B357	11.60	1.89	2.69	18.950	15.634	38.641	10.600	15.4	18.784	15.626	38.565	99.0		0.7047
B359	6.30	1.47	2.44	19.002	15.634	38.693	15.000	25.6	18.767	15.623	38.566	99.0		0.7049
B361	8.00	1.45	7.46	19.108	15.640	38.934	11.700	61.9	18.924	15.632	38.627	118Z		0.7041
B362gab	2.80	0.17	0.49	18.766	15.647	38.565	4.000	11.7	18.704	15.644	38.507	110Z		0.7037
B364	10.68	0.66	5.85	18.953	15.611	38.705	3.996	36.3	18.890	15.608	38.524	110Z		0.7036
B367	23.81	2.03	9.10	19.064	15.641	38.796	5.531	25.4	18.977	15.637	38.670	110Z		0.7066
B369	16.22	1.02	9.17	18.839	15.591	38.606	4.054	37.4	18.776	15.588	38.421	107.5		0.7046
B372	11.14	1.47	8.62	19.316	15.696	38.996	8.618	51.8	19.182	15.689	38.739	99Z		0.7070
B373	11.10	0.98	3.76	18.940	15.669	38.826	5.700	22.5	18.831	15.663	38.691	97Z		0.7052
B381	8.90	0.61	1.82	18.921	15.616	38.618	4.400	13.5	18.837	15.612	38.537	97Z	9.2	0.7051
B385	7.70	0.80	2.79	18.964	15.632	38.712	6.700	24.1	18.836	15.626	38.567	97Z		0.7051
B388	16.90	2.76	10.23	19.109	15.636	38.803	10.600	40.3	18.943	15.627	38.603	130.0	8.2	0.7032
B390	10.90	0.81	5.99	18.963	15.622	38.788	4.800	36.5	18.887	15.619	38.607	107.0	9.6	0.7049
B393gab	1.70	0.20	0.35	18.886	15.616	38.545	7.600	13.6	18.768	15.611	38.477	100.0	7.7	0.7031
B394	9.60	0.87	5.31	18.952	15.647	38.858	5.900	36.8	18.860	15.643	38.676	135.0	10.9	0.7055
B396	17.70	0.91	11.55	18.983	15.628	38.872	3.300	43.4	18.931	15.626	38.657	135.0	10.5	0.7055

Table 3. U, Th, Pb concentrations, initial Pb and Sr isotopic compositions, and $\delta^{18}O$ permil values for whole-rock specimens of plutons of the northern Peninsular Ranges batholith

				WR Present-Day Pb ratios					WR Age-Corrected Pb ratios					
B398	10.10	1.04	8.99	18.985	15.627	38.892	6.700	59.2	18.880	15.622	38.599	135.0	10.0	0.7055
Sample	Pb (ppm)	U (ppm)	Th (ppm)	$^{206}Pb/^{204}Pb$	$^{207}Pb/^{204}Pb$	$^{208}Pb/^{204}Pb$	$^{238}U/^{204}Pb$	$^{232}Th/^{204}Pb$	$^{206}Pb/^{204}Pb$	$^{207}Pb/^{204}Pb$	$^{208}Pb/^{204}Pb$	Age(Ma)	$\partial^{18}O$	Sri
B401												100	8.4	0.7043
B404												100	8.5	0.7040
B406	21.20	2.40	9.62	18.950	15.648	38.752	7.300	30.1	18.835	15.643	38.602	100.0	18.2	0.7133
B407	20.00	2.22	10.59	19.158	15.660	38.881	7.200	35.3	19.045	15.654	38.706	100.0	12.3	0.7066
B408												107.0	8.6	0.7049
B409	11.60	1.76	5.55	19.077	15.620	38.755	9.800	31.8	18.923	15.613	38.597	107.0	8.6	0.7049
B411	7.20	0.73	3.41	18.849	15.603	38.670	6.500	31.4	18.747	15.598	38.515	100	7.4	0.7042
B412	7.70	1.06	2.07	18.928	15.636	38.667	8.900	17.8	18.788	15.630	38.579	100	8.1	0.7042
B413	13.20	2.12	19.49	19.060	15.631	39.038	10.400	98.3	18.897	15.624	38.551	100	9.0	0.7046
B414 gab	1.20	0.42	0.29	18.794	15.597	38.468	22.500	15.9	18.442	15.580	38.388	100	7.2	0.7040
B415												100	10.1	0.7049
B416												100	10.9	0.7052
B418	36.30	2.68	22.54	18.975	15.633	38.806	4.800	41.2	18.900	15.630	38.601	103Z	0.0	0.7055
B420	10.40	1.92	4.20	19.002	15.639	38.725	12.000	26.8	18.829	15.631	38.602	92.5	10.8	0.7054
B422	15.20	4.02	14.09	19.261	15.639	38.958	17.200	62.0	18.970	15.626	38.626	100	9.7	0.7048
B427	6.80	0.69	1.58	18.910	15.621	38.596	6.500	15.3	18.809	15.617	38.521	98.7		0.7045
B429	18.94	2.74	9.99	19.015	15.620	38.716	9.365	35.0	18.868	15.613	38.542	100.0		0.7048
B430	15.30	0.67	5.36	19.044	15.652	38.827	2.800	23.3	18.999	15.650	38.711	100.0		0.7052
B436	14.21	1.10	6.84	18.961	15.632	38.798	5.014	32.0	18.882	15.629	38.639	104.3		0.7047
B439	10.40	1.81	9.05	19.039	15.646	38.917	11.300	57.8	18.863	15.638	38.631	100.0		0.7058
B450	42.20	7.43	39.78	19.306	15.662	39.016	11.500	63.2	19.119	15.653	38.690	104.5	12.3	0.7062
B454	12.90	1.72	10.31	19.130	15.656	38.808	8.700	53.4	18.989	15.650	38.532	104.0	10.8	0.7072
							Santa Ana block							
B458	11.36	1.41	8.27	18.994	15.605	38.769	8.037	48.4	18.843	15.598	38.481	122.0		0.7043
B460	8.50	1.61	7.44	19.221	15.637	38.944	12.300	58.2	18.990	15.626	38.597	124.0	8.3	0.7047
B461	11.37	1.69	7.63	19.091	15.628	38.794	9.643	45.0	18.910	15.620	38.526	119.0		0.7035
B462	12.46	1.69	12.02	19.099	15.617	38.783	8.798	64.2	18.933	15.609	38.401	122.0	8.2	0.7044
B464	11.80	1.59	10.41	19.145	15.646	39.022	8.800	58.9	18.980	15.638	38.671	122.0	8.0	0.7043
B465	14.71	1.75	8.93	19.049	15.614	38.772	7.710	40.4	18.904	15.607	38.532	122.0		0.7036
B466	27.60	1.70	10.44	19.035	15.638	38.807	4.000	25.2	18.960	15.636	38.657	122.0	7.4	0.7040
B470	6.41	3.13	9.46	19.287	15.623	38.951	31.828	98.7	18.689	15.594	38.363	106.3		0.7041
B472	7.12	3.25	9.73	19.246	15.645	39.007	29.767	91.4	18.686	15.618	38.462	124.0		0.7036
B476	8.78	1.79	8.23	19.067	15.626	38.819	13.227	62.4	18.818	15.614	38.448	124.0		0.7036

Table 3. U, Th, Pb concentrations, initial Pb and Sr isotopic compositions, and $\delta^{18}O$ permil values for whole-rock specimens of plutons of the northern Peninsular Ranges batholith

				WR Present-Day Pb ratios					WR Age-Corrected Pb ratios					
Sample	Pb (ppm)	U (ppm)	Th (ppm)	$^{206}Pb/^{204}Pb$	$^{207}Pb/^{204}Pb$	$^{208}Pb/^{204}Pb$	$^{238}U/^{204}Pb$	$^{232}Th/^{204}Pb$	$^{206}Pb/^{204}Pb$	$^{207}Pb/^{204}Pb$	$^{208}Pb/^{204}Pb$	Age(Ma)	$\partial^{18}O$	Sri
B478	9.69	3.14	5.90	19.232	15.602	38.591	20.998	40.5	18.837	15.583	38.350	105.2		0.7038
B480	9.90	1.25	5.85	19.021	15.610	38.736	8.110	38.9	18.868	15.603	38.504	124.0		0.7036
B493	13.26	1.08	3.84	18.797	15.604	38.480	5.239	19.1	18.699	15.600	38.366	124.0		0.7036
B499	10.46	1.56	3.10	18.834	15.604	38.582	9.612	19.6	18.654	15.596	38.465	124.0		0.7036
B500	6.14	0.75	5.04	18.962	15.588	38.575	7.884	54.3	18.813	15.581	38.251	124.0		0.7036
B505 gab	3.10	0.50	0.94	18.785	15.584	38.427	10.400	20.0	18.597	15.575	38.312	117.0	6.9	0.7037
B508												117.0	6.4	0.7036
B509												117.0	5.9	0.7037
B510												124.0	6.5	0.7036
B511gab	3.60	0.40	1.18	18.784	15.578	38.435	7.100	21.6	18.654	15.572	38.311	117.0	6.2	0.7037
B513	4.40	0.70	1.67	18.797	15.581	38.449	10.200	25.0	18.611	15.572	38.305	105.2	6.4	0.7038
B514												105.2	6.2	0.7038
B515												113.4	2.3	0.7036
B516	14.50	1.66	5.33	18.893	15.608	38.621	7.400	24.3	18.730	15.600	38.451	113.4	4.4	0.7036
B517	16.90	2.70	6.98	18.883	15.602	38.550	10.300	27.3	18.656	15.591	38.359	117.0	4.6	0.7036
B518	7.90	1.30	3.32	18.793	15.577	38.419	10.600	27.7	18.628	15.569	38.282	100.0	6.7	0.7036
B519												117.0	6.3	0.7036
B520	9.30	1.64	8.67	18.956	15.598	38.677	11.400	61.8	18.758	15.589	38.338	113.4	5.8	0.7036
B522												105.2	6.6	0.7038
B524	5.60	1.18	4.75	18.858	15.589	37.508	13.600	56.1	18.596	15.577	38.165	117.0	6.3	0.7036
B525												117.0	6.1	0.7036
B530	9.10	1.07	5.24	18.807	15.589	38.496	7.600	38.2	18.676	15.583	38.286	113.4	6.6	0.7036
B531												105.2	6.8	0.7038
B532 gab	4.60	0.55	1.23	18.882	15.597	38.551	7.700	17.7	18.744	15.591	38.450	105.2	6.6	0.7038
B535 gab	4.50	0.74	2.00	18.722	15.586	38.395	10.600	29.3	18.557	15.578	38.250	100.0	6.7	0.7041
B538	6.20	3.32	12.63	19.292	15.609	38.963	34.900	136.2	18.686	15.580	38.213	124.0		0.7036
B540	10.40	1.54	9.89	18.960	15.606	38.686	9.600	63.1	18.793	15.598	38.339	124.0	7.0	0.7036
B546	7.40	0.91	7.05	18.800	15.596	38.709	7.900	63.1	18.684	15.591	38.415	92.5	7.2	0.7043
B556	7.47	1.19	6.68	18.994	15.600	38.701	10.305	48.6	18.842	15.593	38.474	94.0		0.7042
B557	8.30	0.99	2.89	18.912	15.603	38.612	7.698	23.1	18.798	15.598	38.505	94.0		0.7043
				Peninsular Ranges zircon U-Pb age traverse (Premo and others, 1997)										
HSCZ(SA)	7.11	2.57	7.98	19.244	15.649	39.025	23.400		18.785	15.627	38.559	119.0	9.3	0.7054
SMZ (SA)	5.56	3.79	11.42	19.340	15.650	38.950	44.100		18.476	15.608	38.098	120.0	5.9	0.7043

Table 3. U, Th, Pb concentrations, initial Pb and Sr isotopic compositions, and $\delta^{18}O$ permil values for whole-rock specimens of plutons of the northern Peninsular Ranges batholith

SRPZ (SA)	7.11	2.49	6.79	19.246	15.630	38.799	22.600		18.803	15.609	38.404	122.0	8.0	0.7041
PVZ (P)												110.0	7.1	0.7058

				WR Present-Day Pb ratios					WR Age-Corrected Pb ratios					
Sample	Pb (ppm)	U (ppm)	Th (ppm)	$^{206}Pb/^{204}Pb$	$^{207}Pb/^{204}Pb$	$^{208}Pb/^{204}Pb$	$^{238}U/^{204}Pb$	$^{232}Th/^{204}Pb$	$^{206}Pb/^{204}Pb$	$^{207}Pb/^{204}Pb$	$^{208}Pb/^{204}Pb$	Age(Ma)	$\partial^{18}O$	Sri
CZ-1 (P)	10.42	4.28	14.54	19.230	15.654	38.930	26.600		18.773	15.632	38.421	108.0	7.7	0.7047
GZ (P)	7.97	2.03	6.61	19.066	15.669	38.921	16.400		18.784	15.655	38.620	108.0	7.2	0.7044
GZ-1 (P)	8.33	3.31	4.23	19.188	15.636	38.673	25.600		18.747	15.615	38.489	109.0	7.1	0.7041
GZ-2 (P)												113.0	8.8	0.7062
ADTZ (P)												110.0	8.2	0.7059
DVZ (P)												118.0	7.4	0.7042
JMZ (P)	10.85	2.83	4.63	19.023	15.617	38.650	16.700		18.756	15.604	38.507	103.0	7.6	0.7047
MRZ (P)												109.0	8.5	0.7049
VVZ (P)												106.0	7.6	0.7048
BSZ (P)	5.99	0.80	10.10	19.151	15.638	38.910	8.650		19.016	15.632	38.352	98.0	8.6	0.7052
LVZ (P)	6.55	0.86	1.71	19.010	15.633	38.681	8.390		18.876	15.627	38.593	99.0	7.1	0.7050
GATZ (P)	0.46	0.03	0.07	18.851	15.632	38.605	3.740		18.792	15.629	38.556	99.0	7.2	0.7046
SREZ (P)	5.83	0.65	1.69	18.984	15.631	38.645	7.120		18.874	15.626	38.550	99.0	7.9	0.7052
RBZ (P)												99.0	9.6	0.7063
WVRS (P)												97.0	9.0	0.7052
SJZ (SJ)	11.00	1.99	8.11	19.332	15.706	39.086	11.750		19.158	15.698	38.853	94.0	9.9	0.7075
PFZ (SJ)	6.67	1.15	3.36	19.324	15.698	38.966	11.170		19.153	15.690	38.802	98.0	9.7	0.7070
PFZ-1 (SJ)	10.88	3.07	51.20	19.596	15.716	40.230	18.660		19.340	15.704	38.827	84.0	8.3	0.7078
PHZ (SJ)	17.19	2.31	12.58	19.523	15.728	39.192	8.780		19.402	15.722	38.977	83.0	9.1	0.7080

Notes : Sample locations and rock names are given in Table 1. Ages and Sri values are from Table 2.